PAPER

Assessing the advantages of 3D bioprinting and 3D spheroids in deciphering the osteoarthritis healing mechanism using human chondrocytes and polarized macrophages

To cite this article: Nilotpal Majumder *et al* 2024 *Biomed. Mater.* **19** 025005

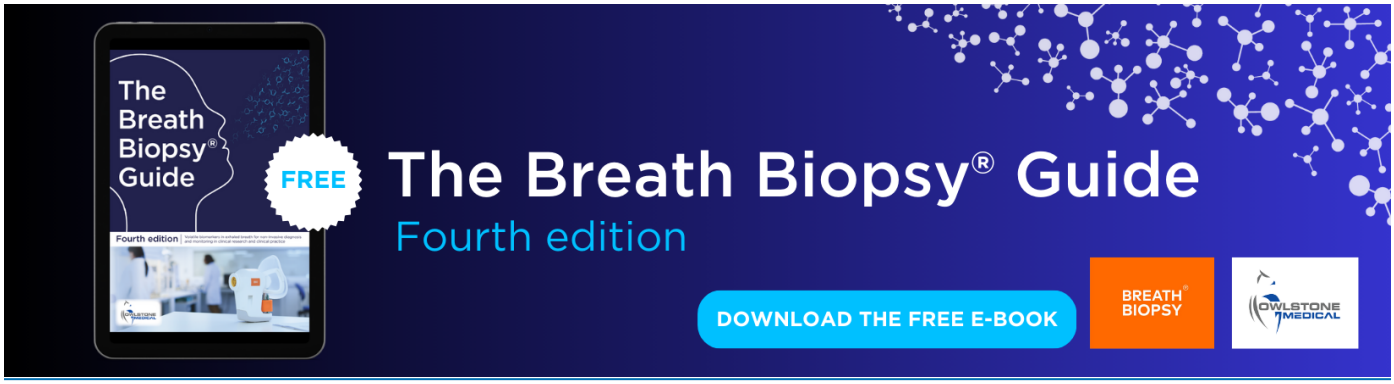

IOP Publishing Biomed. Mater. 19 (2024) 025005 https://doi.org/10.1088/1748-605X/ad1d18

Biomedical Materials

PAPER

RECEIVED
3 July 2023

REVISED
5 January 2024

ACCEPTED FOR PUBLICATION
10 January 2024

PUBLISHED
19 January 2024

Assessing the advantages of 3D bioprinting and 3D spheroids in deciphering the osteoarthritis healing mechanism using human chondrocytes and polarized macrophages

Nilotpal Majumder[1], **Subhadeep Roy**[1], **Aarushi Sharma**[1], **Shuchi Arora**[2], **Raju Vaishya**[3], **Amitabha Bandyopadhyay**[2] **and Sourabh Ghosh**[1,*]

[1] Regenerative Engineering Laboratory, Department of Textile and Fiber Engineering, Indian Institute of Technology, New Delhi 110016, India
[2] Department of Biological Sciences & Bioengineering, Indian Institute of Technology, Kanpur 208016, India
[3] Indraprastha Apollo Hospitals Delhi, New Delhi 110076, India
[*] Author to whom any correspondence should be addressed.

E-mail: sghosh08@textile.iitd.ac.in

Keywords: osteoarthritis, primary chondrocytes, M2 macrophage, 3D spheroid, 3D bioprinting

Supplementary material for this article is available online

Abstract

The molecular niche of an osteoarthritic microenvironment comprises the native chondrocytes, the circulatory immune cells, and their respective inflammatory mediators. Although M2 macrophages infiltrate the joint tissue during osteoarthritis (OA) to initiate cartilage repair, the mechanistic crosstalk that dwells underneath is still unknown. Our study established a co-culture system of human OA chondrocytes and M2 macrophages in 3D spheroids and 3D bioprinted silk-gelatin constructs. It is already well established that Silk fibroin-gelatin bioink supports chondrogenic differentiation due to upregulation of the Wnt/β-catenin pathway. Additionally, the presence of anti-inflammatory M2 macrophages significantly upregulated the expression of chondrogenic biomarkers (COL-II, ACAN) with an attenuated expression of the chondrocyte hypertrophy (COL-X), chondrocyte dedifferentiation (COL-I) and matrix catabolism (MMP-1 and MMP-13) genes even in the absence of the interleukins. Furthermore, the 3D bioprinted co-culture model displayed an upper hand in stimulating cartilage regeneration and OA inhibition than the spheroid model, underlining the role of silk fibroin-gelatin in encouraging chondrogenesis. Additionally, the 3D bioprinted silk-gelatin constructs further supported the maintenance of stable anti-inflammatory phenotype of M2 macrophage. Thus, the direct interaction between the primary OAC and M2 macrophages in the 3D context, along with the release of the soluble anti-inflammatory factors by the M2 cells, significantly contributed to a better understanding of the molecular mechanisms responsible for immune cell-mediated OA healing.

1. Introduction

Osteoarthritis (OA) is characterized by extensive cartilage degeneration and subchondral bone damage marked by an overwhelming inflammatory response in and around the surrounding joint microenvironment [1–3]. The pathophysiology of OA is multifactorial, involving the participation of different immune cells and their respective secreted paracrine factors that mediate the disease severity and progression [3]. Although most of the research is conducted to decipher ways to halt OA, the underlying molecular mechanisms that govern the onset and suppression of OA are still unclear.

Cartilage degradation is commonly associated with chronic inflammation involving the active participation of macrophages in different polarized states [4–6]. The role of these macrophages in OA progression and suppression has been extensively elucidated by Chen *et al* [7] and Fernandes *et al* [8]. The resident tissue macrophages polarise into classically (M1) or alternatively (M2) activated

macrophages based on environmental cues, surrounding cytokine microenvironment, and recruitment of circulating monocytes [9, 10]. The activated pro-inflammatory M1 macrophages secrete various inflammatory cytokines (IL-1β, TNF-α, IL-6, IL-8) that influence the chondrocytes to produce chondrogenic matrix-degrading enzymes (MMP-13, ADAMTS5) creating an inflammatory microenvironment within the joint tissue. However, M2 macrophages possess an anti-inflammatory potential capable of reversing OA progression as well as promoting healthy tissue regeneration [4, 11, 12]. The metabolism of M2 macrophage [13] involves the release of anti-inflammatory IL-4, IL-10, IL-13, and arginase-1, which can alter OA degradation mechanisms [14–16]. These immune cells act as reservoir bases contributing to cartilage homeostasis and regeneration [10, 17, 18]. The chemical cues from the residing macrophages mediate the infiltration of the circulating monocytes to replace the pro-inflammatory macrophages and initiate healing in an inflammatory OA microenvironment [19, 20].

Our research group has extensively explored silk fibroin-based biomaterial blends and 3D bioprinting technology to generate 3D neo-cartilage tissue constructs using different cell types. However, standalone silk protein putatively lacks adequate cell binding motifs and displays Newtonian behavior during rheology, making it non-printable and less cytocompatible [13]. Hence, we performed considerable research to blend gelatin into the silk solution to impart shear-thinning behavior, an essential requirement for smooth extrusion during 3D bioprinting, as well as additional cell attachment motifs [21]. In that context, Das *et al* demonstrated successful re-differentiation of primary articular chondrocytes when 3D bioprinted with an appropriate proportion of silk fibroin and gelatin (SF-G) and incubated in chondrogenic media for a period of 28 d [22]. The same SF-G composite, when enzymatically crosslinked with mushroom tyrosinase, encapsulated with human nasal turbinate-derived mesenchymal stem cells and 3D bioprinted, depicted high cell viability (28 d) as well as enhanced chondrogenesis [23]. Chamettachal *et al* and Chawla *et al* utilized the chondro-stimulatory role of the SF-G blend in deciphering the underlying signaling pathways responsible for enhanced chondrogenesis using human-derived mesenchymal stem cells and articular chondrocytes [24, 25]. Additionally, they illustrated the cell-ECM interaction required for chondrogenic differentiation, besides demonstrating the drastic reduction of chondrocyte hypertrophy in silk-gelatin bioink. The pro-chondrogenic role of 3D bioprinted SF-G bioink-based constructs has been exquisitely demonstrated by Chawla *et al* through an extensive proteomic analysis confirming the upregulation of Wnt signaling pathway, a key modulator of *in vitro* chondrogenesis [25]. Thus, these studies utilize the concept of auxiliary cell-type involvement in OA phenotype development and establishment of cell-ECM communication using a wide array of biomaterials to understand the disease severity and further devise therapeutic strategies to suppress the progression [21, 26, 27].

In a co-culture setup, the macrophage or its secreted factors can control the activity of the recruited cartilage-specific cell types in a programmed manner while maintaining its stable phenotype. One such paracrine influence of macrophage-secreted factors on chondrocytes was investigated by Sun *et al* [28]. They developed an *in vitro* 3D OA model in silk-based scaffolds with articular chondrocytes primed with a macrophage conditioning medium that demonstrated exorbitant OA characteristics with marked expressions of collagen X (COL-X) and chondrocyte apoptosis. Alternatively, the chondro-stimulatory role of M2 macrophages was reviewed by Fernandes *et al,* underlining the direct correlation between the secretion of pro-chondrogenic cytokines (TGF-β) by stable M2 macrophages and collagen production [8]. A study by Fujihara *et al* demonstrated the role of Fas ligand (FasL) present in murine chondrocytes to inhibit the infiltration of classically activated M1 macrophages, creating an 'immune-privilege' site [29]. Reports from their study also revealed a higher extent of cartilage maturation (enhanced GAG production) in the implanted auricular chondrocyte embedded l-poly l-Lactic acid scaffolds in FasL-positive mice models with reduced macrophage infiltrations. Samavedi *et al,* however, developed a 3D co-culture system using classically activated macrophages (M1) and chondrocytes both embedded in separate poly (ethylene glycol) diacrylate hydrogel in a transwell-based system to simulate an OA joint microenvironment [30]. The culture platform with osteoarthritic chondrocytes (OAC) and M1 macrophages displayed maximum OA characteristics marked by enhanced expression of IL-1β, VEGFA and MMPs. Furthermore, the same chondrocytes cultured in the transwell platform with non-activated macrophages demonstrated redundant expression of the pro-inflammatory cytokines. Thus, the results from their study highlighted the role of macrophages in both OA progression as well as suppression. However, the major limitation of their study lies in the absence of direct contact between both cell types besides continuous replenishment of the macrophage-encapsulated hydrogel discs every two days for the maintenance of stable M1 phenotype, making the protocol physiologically irrelevant concerning the macrophage-mediated evaluation of OA suppression. Additionally, the co-culture study was carried out only for a period of 6 days without any prior re-differentiation of the isolated chondrocytes

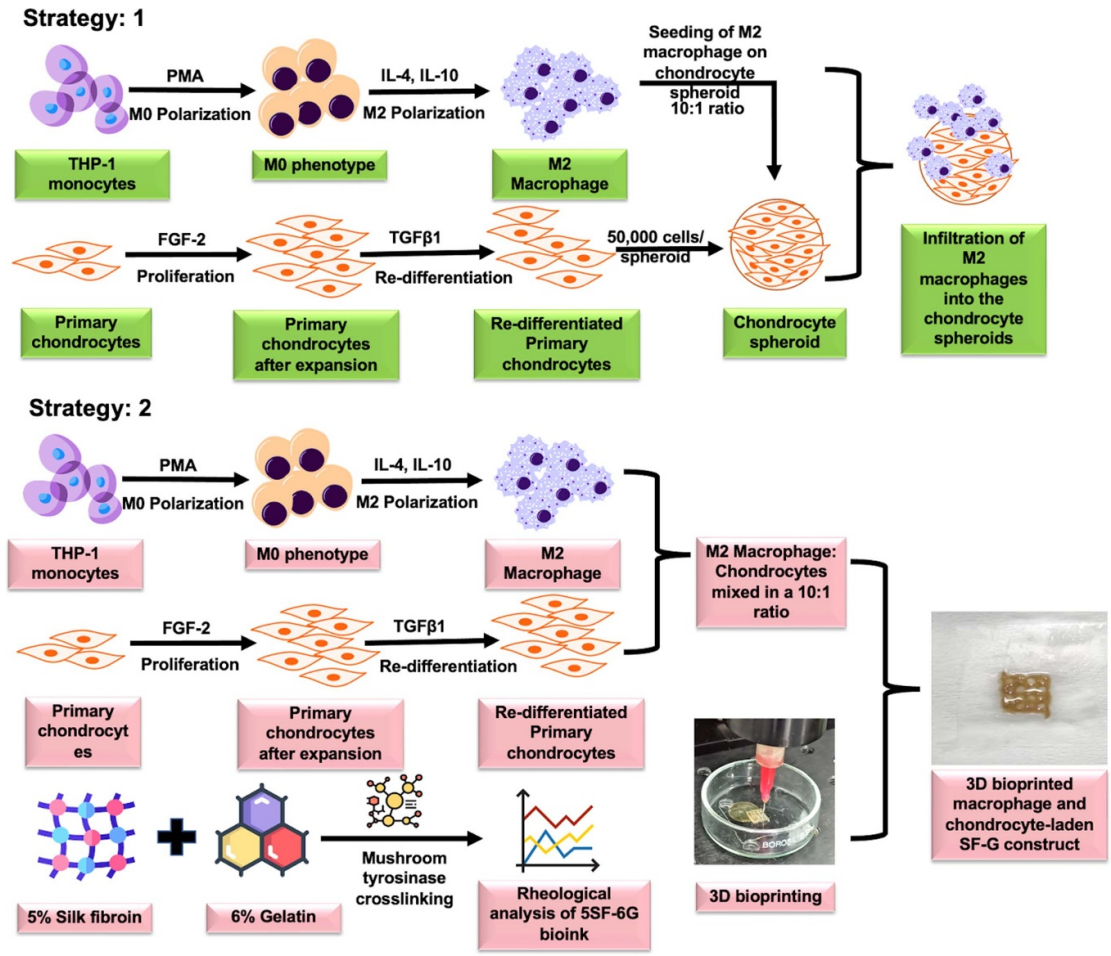

Figure 1. A detailed schematic diagram summarizing the experimental plan of the research.

as *in vitro* expansion only contributes to cellular dedifferentiation [31, 32].

All the studies mentioned above underlining the chondroprotective role of M2 macrophage phenotype in promoting cartilage repair while suppressing OA have been described either using macrophage-conditioned media or transwell culture systems. Such indirect communication fails to mimic the native infiltration of the circulating synovial macrophages into the OA microenvironment. Moreover, using RAW 264.7 macrophages (murine origin) and chondrocytes (human origin) from two different species significantly minimized the effectiveness of the signaling crosstalk between the two. Additionally, none of the studies have considered simulating the direct cell-cell and cell-ECM interaction present in the OA cartilage microenvironment of the knee joint. Therefore, in this current study, we attempted to replicate a healing OA microenvironment comprising a 3D co-culture setup of human primary osteoarthritic chondrocytes (OACs) and human M2-macrophages in a 3D spheroid-based vs. 3D bioprinted model and compared the efficacies of both the culture systems using different experimental analyses (figure 1). The primary objective of this study is to accentuate the role of M2-macrophages in promoting neo-cartilage regeneration while blocking the progression of OA in the co-culture system with and without exogenous anti-inflammatory interleukin (IL) supplementation. Moreover, through this study, we aim to answer the following questions:

1. Is it possible to mimic the *in vivo* direct interaction between the M2 macrophage and OACs in an *in vitro* co-culture setup?
2. Which of the two 3D models (3D spheroid or 3D bioprinted constructs) served better in understanding the mechanism for minimizing OA symptoms, promoting chondrogenesis and allowing stable maintenance of M2 macrophage phenotype?
3. Is it essential to prime the culture media with anti-inflammatory ILs to achieve stable anti-inflammatory M2 phenotype in the 3D culture systems?
4. Is there any direct correlation between the M2-macrophage phenotype polarization and cartilage homeostasis?

Our study attempted to answer these questions by evaluating different groups in both human cell-based spheroid models and 3D bioprinted silk-gelatin constructs, with or without Interleukin (IL) supplementation and macrophage infiltration. The 3D spheroid-based platform was primarily designed to observe direct inter-cellular interaction between the human macrophages and human chondrocytes, whereas the 3D bioprinted constructs successfully recapitulated the complex cell-ECM interaction required to activate several signaling pathways to promote neo-cartilage formation [23, 27, 33]. The isolated OACs were initially expanded and further re-differentiated for a period of 14 days to encourage chondrogenic traits before establishing the co-culture model with M2 macrophages for another 10 days. The extent of chondrogenesis, OA suppression and M2 phenotype maintenance in both 3D spheroid and 3D bioprinted models were investigated by performing a widespread gene and protein expression analysis of different chondrogenic, hypertrophic and macrophage surface markers. We further assessed the release of macrophage-mediated chemokines to identify the oxidative defense machinery under diseased conditions. The rationale behind our study was to mimic the direct interaction between the M2 macrophages and the prevailing OACs in the OA microenvironment to initiate chondrocyte healing. Therefore, this study helped us unravel the influential role of resident M2 macrophages in OA suppression.

2. Materials and methods

2.1. Materials

The RPMI-1640 medium (Cat. No.- 1875 093, Gibco), DMEM (Cat. No. 11 965–092, Gibco), HEPES buffer (Cat. No. TCL021; HiMedia) and sodium bicarbonate (Cat. No. 11 360–070, Gibco) and glutamine (Cat. No. TCL012; Himedia) and penicillin–streptomycin–glutamine (PSG; Cat. No. 10 378 016, Gibco), foetal bovine serum (FBS; Cat. No. 10 438–026, Gibco), and collagenase type-2 (Cat. No. 17 101–015 Gibco), phosphate-buffered saline (PBS; Cat. No. SH30256.01; HyClone), antibiotic/antimycotic (AB/AM) solution (Cat. No. SV30079.01, Hyclone) and insulin–transferrin–selenium (Cat. No. 41 400–045, Gibco) and linoleic acid-albumin (Cat. No. L9530, Gibco), Ascorbic acid 2-phosphate (Cat. No. A8960, Gibco), dexamethasone (Cat. No. D4902; Gibco) and fibroblast growth factor (FGF)-2 (cat. No. GTX29596-pro; Gentex), TGF-β1 (Cat. No. GTX00101-pro, Gentex) and TGF-β3 (Cat. No. GTX48128-pro, Gentex) and poly—(hydroxyethyl methacrylate) (poly-HEMA) (Cat. No. P3932; Sigma-Aldrich), phorbol 12-myristate 13-acetate (PMA) (Cat. No. P8139; Sigma-Aldrich) and IL-4 (Cat. No. TC362; HiMedia) and IL-10 (Cat. No. TC424, Himedia), and RNeasy Mini Kit (Cat. No.-74 104, Qiagen), and a cDNA synthesis kit (Cat. No. K1621; Thermo Scientific), SYBR Green master mix (Cat. No. 204 145, Qiagen), and primary antibody, COL-1 (Cat. No. PA1-85 319; Invitrogen), and COL-II (Cat. No. CIIC1, DSHB), and primary antibodies, COL-X (Cat. No. X-AC9, DSHB), and the primary antibody CD-14 (Cat. No. MA1-23 611; Invitrogen), and the primary antibody CD-36 (Cat. No. MA5-14 112; Invitrogen), and the primary antibody CD-163 (Cat. No. TA506380; Origene), Alexa Fluor 488 (Cat. No. A11008; Invitrogen), Alexa Fluor 594 (Cat. No. 35 562, Invitrogen), and the TBARS assay kit (Cat. No. CCK023 EZ Assay, Himedia), GST assay kit (Cat. No. CCK028 EZ Assay, Himedia), antioxidant assay kit (Cat. No. CCK071 EZ Assay, Himedia) and nitric oxide (NO) (Cat. No. CCK061, EZ Assay, Himedia).

2.2. Cell culture

2.2.1. Collection of OA and healthy cartilage

Healthy and osteoarthritic articular cartilage samples ($N = 3$) were collected from patients undergoing knee arthroscopy and Total knee arthroplasty, respectively, at Indraprastha Apollo Hospital, New Delhi. Institutional ethics committee approval was obtained (IAH-BMR-018/10-19), and informed consent was obtained from all participants before the initiation of the study. For healthy articular cartilage (HC), a single 5 mm diameter osteochondral biopsy was collected during surgery from the non-load-bearing area using a biopsy needle. For OAC, both femur and tibia sides were collected, and a 5 mm diameter osteochondral biopsy was performed in the laboratory.

2.2.2. Isolation, expansion, and re-differentiation of chondrocytes from human cartilage biopsies

Freshly collected HC and OAC were first washed with PBS–PSG solution and kept for sterility checks for three days in a complete medium at 37 °C under a 5% CO_2/95% air atmosphere. The minced cartilage chips were then processed for enzymatic digestion using 0.15% collagenase type-2 (10 ml of solution per gram of cartilage chips) for 22 h at 37 °C. The cells were then kept for expansion in DMEM enriched with 10% FBS, 1% Antibiotic Antimycotic solution, 1 mM sodium pyruvate, 100 mM HEPES buffer, 0.29 mg ml^{-1} L-glutamine, 5 ng ml^{-1} FGF-2 [34]. Following this, the chondrocytes were subjected to re-differentiation protocol in DMEM/F-12 supplemented with 1% sodium pyruvate, 1% HEPES, 1% Antibiotic-Antimycotic, 1% ITS + premix, 10 ng ml^{-1} TGF-β3, 10^{-7} M Dexamethasone and 0.1 mM Ascorbic acid phosphate for a period of 14 days.

2.2.3. The proliferation and differentiation of monocytes

THP-1 cells were collected from the National Centre for Cell Science, Pune, and henceforth referred to as monocytes. Monocytes were cultured in RPMI-1640 medium supplemented with 1% Antibiotic-Antimycotic solution and 10% heat-inactivated FBS. Monocytes were differentiated into M0 macrophages using 200 nM PMA with 1% Antibiotic Antimycotic solution and 10% heat-inactivated FBS. After incubation for 10 d, monocytes were differentiated into M0 macrophages [35]. M0 macrophages were then cultured using 200 ng μl^{-1} IL-4 and 200 ng μl^{-1} IL-10 in 1% Antibiotic-Antimycotic solution, 10% heat-inactivated FBS, and RPMI-1640 medium. The cells were incubated at 37 °C in a 5% CO_2/95% air atmosphere. After incubation for 5 days, M0 macrophages successfully differentiated into M2 macrophages [36]. The combination of IL-4 and IL-10 is referred to as an IL.

2.3. Preparation of silk-based bioink

2.3.1. Preparation of silk solution

Silk fibroin was successfully isolated from *Bombyx mori* silk cocoons, as described in our previous studies [37, 38]. Briefly, 5 grams of silk cocoons were cut into small pieces and treated with 0.02 M Na_2CO_3 for 30 min at 100 °C. The obtained silk fibers were washed with deionized water and air-dried. Silk fibroin fibers were then dissolved in 9.3 M lithium bromide solution at 60 °C for 4 h. The dissolved fibroin solution was dialyzed against deionized water for 48 h, and the collected silk solution was weighed and stored at 4 °C for further use.

2.3.2. Preparation of bioink

The silk-gelatin bioink was prepared as described in our previous study [25, 39]. Gelatin was disinfected by overnight incubation in 100% ethanol, followed by air drying under sterile conditions. Silk fibroin was sterilized in an autoclave. A 6% (w/v) gelatin solution was prepared using 10% 10*X* medium and 10% FBS. The final volume was 600 µl with 5% (w/v) SF solution and incubated at 37 °C for 15 min to prepare the final blend of 5% Silk-6% Gelatin (SF-G) [40]. After preparing a homogenous blend of SF-G, 750 kU ml^{-1} of mushroom tyrosinase was added to induce enzymatic crosslinking.

2.3.2.1. Experimental design

Freshly isolated HCs and OACs were cultured to form a three-dimensional (3D) model. For each experimental set, we first developed a 3D microcartilage model [34]. HC spheroids were used as controls in all experiments. The 3D OA microcartilage model was cultured under four different conditions:(1) without ILs, (2) with ILs, (3) with only M2 macrophages, and (4) with M2 macrophages and ILs. Spheroids were harvested on days 3, 7, and 10.

2.3.3. Formation of cell spheroids

For the development of cell spheroids, both HC and OA chondrocytes, 0.5×10^5 cells were seeded in poly-HEMA coated 96-well U-bottom plates [33, 34]. The cells were incubated in a complete medium for 3 days. After the formation of cell spheroids, the spheroids were transferred to a chondrogenic differentiation medium for the formation of healthy chondrocyte spheroids. The components of the chondrogenic differentiation medium were 1.25 µg ml^{-1} insulin-transferrin-selenium, 4.7 µg ml^{-1} linoleic acid with albumin, supplemented with 0.1 mM ascorbic acid 2-phosphate, 10^{-7} M dexamethasone and 10 ng ml^{-1} TGF-β3. The cell spheroids were cultured for 14 days to form a stable cartilage model. Furthermore, the OAC spheroids were cultured in a hypertrophic medium with components similar to a chondrogenic medium with an additional 50 nM L-thyroxine to generate OAC spheroids.

2.3.4. M2 macrophage seeding on cell spheroids

M2 macrophages were seeded directly onto OA cell spheroids at a ratio of 10:1 [41]. After the addition of M2 macrophages to the stable OA microcartilage, the medium for further experiments was replaced with RPMI-1640 under all conditions. The spheroids were incubated at 37 °C in a 5% CO_2/95% air atmosphere, and the OA and HC spheroids were harvested on days 3, 7, and 10.

2.3.5. Development of 3D bioprinted OA chondrocytes and M2 macrophage model

Freshly isolated OA chondrocytes were encapsulated in a silk–gelatin-based bioink and processed for 3D bioprinting at 23 °C. The 3D bioprinted OA chondrocytes were studied as a control set for the entire experiment. OA chondrocytes were co-cultured with M2 macrophages at a ratio of 10:1 [41]. The 3D bioprinted constructs were further cultured under two different conditions: (1) without ILs and (2) with ILs. The constructs were harvested on days 3, 7, and 10.

2.4. Gene expression

The total RNA was extracted from the 3D spheroids and 3D bioprinted constructs comprising OACs and M2 macrophages using an RNeasy mini kit (Qiagen, India) as per the instructions given in the manufacturer's protocol. Samples were harvested on days 3, 7 and 10 for both 3D spheroid and 3D bioprinted systems. The first-strand cDNA synthesis kit was used to reverse-transcribe the isolated RNA. Quantitative RT-PCR was performed using SYBR Green Master Mix and a Rotor-Gene Q thermocycler (Qiagen, Hilden, Germany). Quantitect primers were used to investigate the gene expression of COL-I, COL-II,

COL-X, MMP-1, MMP-3, and MMP-13 to assess chondrogenesis and hypertrophy in the OA microcartilage. HC spheroids were used as controls on day three. To investigate the dedifferentiation of M2 macrophages in OA microenvironment, gene expression analyses of CD-14, CD36, CD68, IL-4, and IL-10 were performed. The gene expression profile was compared with the 3D bioprinted construct in three different culture conditions (OAC, OAC + M2, OAC + M2 + IL). M2 macrophages were used as controls in 2D culture. GAPDH served as the housekeeping gene for all the sample sets. All reactions were performed in triplicates.

2.5. Immunofluorescence studies

All spheroids were collected at their respective time points (days 3 and 10) and fixed overnight in 4% formaldehyde at 4 °C. After overnight fixation, spheroids and 3D bioprinted constructs were washed with PBS and stored for antigen retrieval. Each primary antibody was subjected to a different antigen-retrieval process. For COL-I, chemical-based antigen retrieval was performed using a sodium citrate buffer at 95 °C for 10 min. For COL-II and COL-X, enzymatic antigen retrieval was performed using pepsin at 37 °C for 30 min. For CD-14, CD-68, and CD-163, Hydrogen peroxide was used for antigen retrieval. The spheroids were then treated with 3% hydrogen peroxide for 2 min. After antigen retrieval, spheroids were blocked. Blocking was performed for 40 min in heat-inactivated goat serum solution in 0.05% Triton X-100 in PBS at room temperature. After blocking, spheroids were incubated overnight at 4 °C with their respective primary antibodies. The dilutions used were COL-I (1:100), COL-II (1:20), COL-X (1:20), CD-14 (1:100), CD-68 (1:100), and CD-163 (1:100). After incubation, the spheroids were rinsed three times with 0.05% Triton X-100 in PBS. The spheroids were then incubated with secondary antibodies labeled with Alexa Fluor 488 and Alexa Fluor 546 in the dark for 4 h at room temperature in PBS (1:250 dilution). The cells were rinsed with PBS and stained with DAPI (1:1000) in PBS for 2 min to stain nuclei. Negative controls were performed during each analysis by omitting the primary antibodies. Fluorescence images were acquired using a LSM 780 confocal microscope (Zeiss, Jena, Germany). The Zen-Black version was used for image processing [42, 43].

2.6. Release assay of chemokines into the medium

2.6.1. Estimation of antioxidants in the medium

Antioxidant activity was estimated according to the manufacturer's instructions using an EZ Assay™ Antioxidant Activity Estimation Kit. According to this principle, the ferric ion-chromogen complex is reduced to colored ferrous ions at low pH. The media of OAC spheroids under all four conditions on days 3, 7, and 10 were compared with those of HC spheroids. The medium was plated in triplicate using Trolox standards and a blank. The FRAP values were obtained by comparing the absorbance change at 593 nm in test reaction mixtures containing ferrous ions at known concentrations [44].

2.6.2. Lipid peroxidation in the TBARS medium

The lipid peroxidation was estimated according to the manufacturer's instructions using the EZ Assay™ TBARS assay kit. This assay was performed to estimate lipid peroxidation in cells based on the reaction of MDA with the chromogenic agent thiobarbituric acid to form the MDA-TBA adduct (1:2). Calcium serves as an indicator of oxidative stress in cells following calcium supplementation. Absorbance was directly proportional to the concentration of TBARS in the samples. The media of OAC spheroids under all four conditions on days 3, 7, and 10 were compared to those of HC spheroids. This complex has an absorption maximum of 532 nm and can be measured spectrophotometrically between 530 nm and 540 nm [45].

2.6.3. Protein–protein interaction by STRING analysis

The networks were made and looked at with Cytoscape software (version 3.8.0). Genemania's (http://genemania.org/) connectivity for the building network in Cytoscape helps identify how proteins interact with each other and how cytokines work as a network. Lastly, we found the top targets with node degrees that were not too low. Tools that look for genes that interact with each other (STRING; http://string-db.org) (version 10.0) were used to predict PPI networks.

2.7. Statistical analysis

Statistical analysis was performed using the GraphPad Prism 7 software (San Diego, CA, USA). One-way analysis of variance (ANOVA) followed by Bonferroni multiple comparison tests was used for gene expression analysis and biochemical assays. Data are presented as mean ± SD. All experiments were performed twice in biological triplicate to monitor the performance of each experimental set.

3. Results

3.1. Morphological changes in 3D spheroids

From the bright field microscopic images, the HC are characterized by their sparse distribution and less fibroblastic morphology (polygonal shaped) with negligible cytoplasmic extensions at the same time point when cultured in 2D (figure 2(A)). However, the OACs are marked with fibroblastic morphology when cultured in a monolayer with increased proliferation, cell–cell communication and extensive

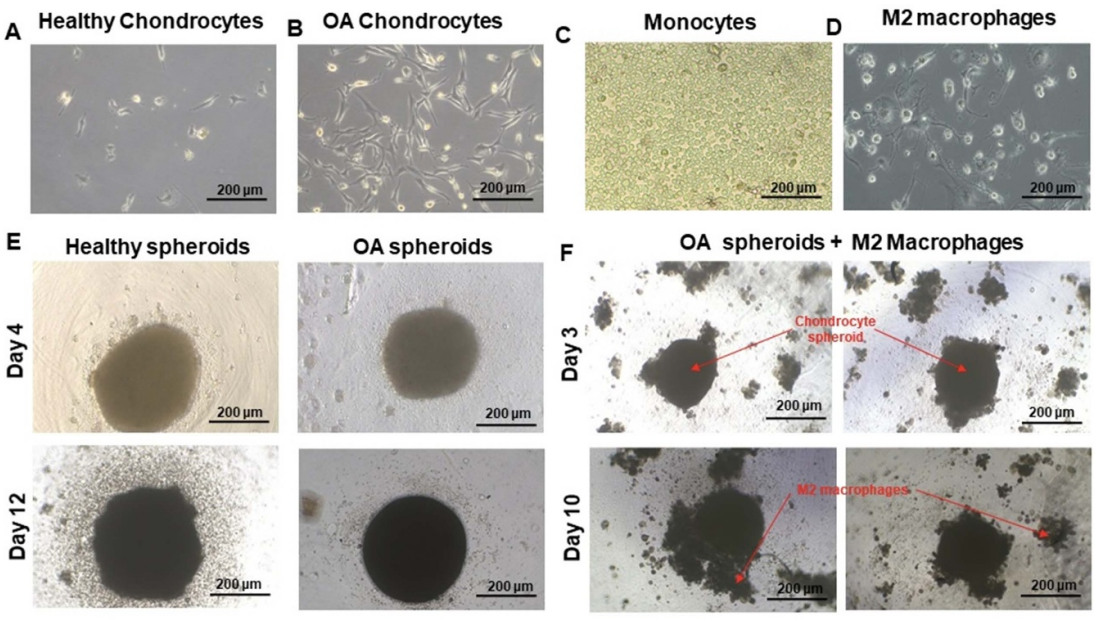

Figure 2. Representative phase-contrast images to show (A) morphology of healthy and (B) OA chondrocytes proliferated in monolayer culture. (C) Healthy THP-1 monocytes, (D) Polarized M2 macrophage, (E) Healthy and OAC spheroids at day 4 and 12 of culture and (F) Depicting the interaction between OAC spheroids and M2 macrophages on day 3 and day 10.

filopodia formation (figure 2(B)). Similarly, the monocytes display a round mononuclear morphology due to their non-adherent nature. In contrast, the M2 macrophage was found to adhere to the flask with stretched and elongated morphology, with extracellular projection (figures 2(C) and (D)). Both healthy and OA spheroids retained intact spheroidal structures after 12 days of culture (figure 2(E)). The direct interaction of M2 macrophage with OA spheroid was evident on day 3, which subsequently increased on day 10 (figure 2(F)).

3.2. Gene expression analysis

3.2.1. Gene expression analysis of cartilage-specific genes

The gene expression analysis was conducted to investigate chondrogenesis and OA suppression in the 3D spheroid and 3D bioprinted co-culture models. The extent of chondrogenic regeneration, along with chondrocyte dedifferentiation, hypertrophy, and matrix remodeling, was studied by evaluating the expressions of COL-II, collagen-I (COL-I), collagen-X (COL-X) and matrix metalloproteinases (MMP-1 and MMP-13) as markers for three different time points (days 3, 7 and 10). The different groups used in the study have been listed in table 1.

When comparing the gene expression of all the experimental groups of the 3D spheroid model, the maximum expression of **COL-II** was recorded on day 10 for all groups (figure 3(A)). The only OAC spheroid group demonstrated a decline in COL-II expression (9.25-fold, $p < 0.01$) compared to the HC microcartilage model on day 10, which increased slightly (2.69-fold, $p < 0.01$) upon the addition of exogenous ILs (IL-4 and IL-10). The OAC spheroids, when co-cultured with M2 macrophage without any exogenously added ILs, however, demonstrated a 6.16-fold increase in COL-II expression ($p < 0.01$) than the OAC spheroid group, illustrating the role of M2 macrophages in promoting collagen secretion during chondrogenesis. However, when the OACs and M2 macrophages were co-cultured within a 3D bioprinted construct, the COL-II expression escalated 7.66-fold ($p < 0.01$) than the 3D spheroid OAC group. Moreover, a higher trend in COL-II expression has been observed in the 3D bioprinted group than in the 3D spheroid group for the OAC and M2 co-culture model on day 10 (with and without ILs), signifying the pro-chondrogenic role of silk fibroin-gelatin microenvironment in stimulating chondrogenesis. The OAC + M2 3D spheroid and 3D bioprinted group with ILs depicted sufficient chondrogenic regeneration marked with a 4.44-fold and 3.42-fold increase in COL-II expression than their respective OAC control groups but comparatively less than the only OAC + M2 group.

Table 1. Experimental groups.

3D spheroids	3D bioprinted constructs
HC spheroid	3D bioprinted OAC
OAC spheroid	
OAC spheroid + M2	3D bioprinted OAC + M2
OAC spheroid + IL	
OAC spheroid + M2 + IL	3D bioprinted OAC + M2 + IL

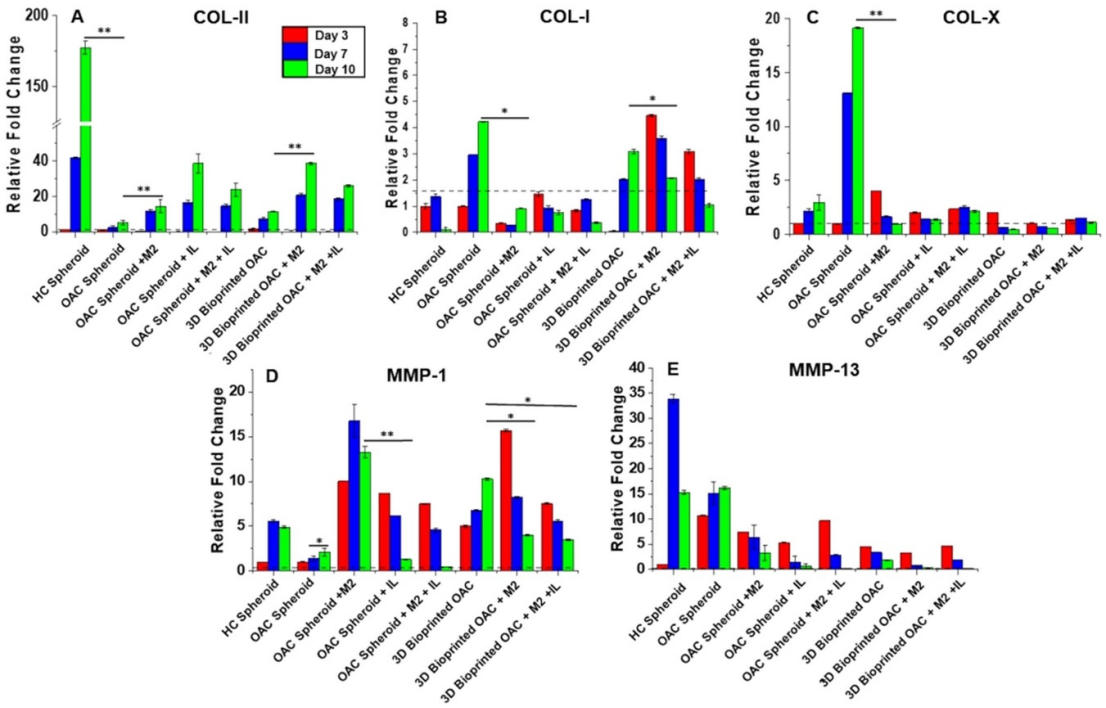

Figure 3. Quantitative real-time PCR to evaluate gene expression of (A) COL-II, (B) COL-I, (C) COL-X, (D) MMP-1 and (E) MMP-13 at days 3, 7 and 10 of HC spheroids, OAC spheroids, OAC spheroids + IL, OAC spheroids + M2, OAC spheroids + M2 + IL, OAC 3D bioprinted, OAC + M2 3D bioprinted and OAC + M2 + IL 3D bioprinted to evaluate the regeneration, de-differentiation, hypertrophy and matrix remodeling of HC. The horizontal black dotted line indicates the expression of the control samples, i.e. M2 macrophages. Values are mean ± SD; $n = 3$/group. Symbol * indicates $p < 0.05$ and ** indicates $p < 0.01$." Data normalized to GAPDH.

The onset of chondrocyte hypertrophy during chondrogenic differentiation of the 3D spheroid and 3D bioprinted models was evaluated with the expression of chondrocyte dedifferentiation marker **COL-I** and hypertrophy-inducing marker **COL-X** (figures 3(B) and (C)). The OAC + M2 3D spheroid group demonstrated a sharp decline in COL-I expression (5.63-fold, $p < 0.05$) at day 10, similar to the 3D bioprinted group (1.49-fold, $p < 0.05$) when compared against their only OAC counterparts (OAC spheroid and 3D bioprinted OAC). This concept was further highlighted when adding ILs in the OAC spheroid group mitigated the COL-I expression by 4.65-fold. An elevated expression level of COL-I was observed at all time points for the OAC group that depicted an increasing trend from day 3 to day 10, while negligible expression was observed in the case of HC spheroids. A similar trend was also observed for the expression of hypertrophic differentiation marker COL-X. The OAC spheroid group showed an upregulation in the expression profile of COL-X from day 3 to day 10, which was subsided by 19-fold on day 10 with the addition of anti-inflammatory ILs (OAC spheroid + ILs). Similarly, when the anti-inflammatory M2 macrophages were co-cultured with primary OACs in both 3D spheroid and 3D bioprinted systems, a negligible expression of COL-X (p not significant) was observed at day 10 for both groups at all time points. However, the OAC + M2 3D bioprinted group showed a greater decrease (2.4-fold, $p < 0.001$) than the OAC + M2 spheroid group at day 10, demonstrating the upper hand of the 3D bioprinted co-culture platform in abrogating hypertrophy. The exogenous addition of ILs, however, did not significantly alter the expression profile of COL-X from day 3 to day 10 in both the culture systems. However, the 3D spheroid denoted a comparatively 1.89-fold higher level of COL-X than the 3D bioprinted, highlighting their tendency towards hypertrophy. A noteworthy observation is the nominal level of COL-X expression in the 3D bioprinted OAC group. A plausible reason could be the chondro-stimulatory role of the silk fibroin gelatin matrix, which majorly contributed to the redundant expression of COL-X in this group.

The extracellular matrix degradation during chondrogenesis was assessed using the expression of matrix-degrading enzymes **MMP-1** and **MMP-13** (figures 3(D) and (E)). These MMPs are secreted by the cells in response to external stimuli such as cytokines and growth factors. The expression pattern of MMP-1 in OAC spheroids depicted an increasing trend (2.1-fold, $p < 0.05$) from day 3 to day 10. The addition of ILs to the OAC spheroid group displayed an increasing trend from day 3 to day 7, followed by its downregulation on day 10, similar to the HC

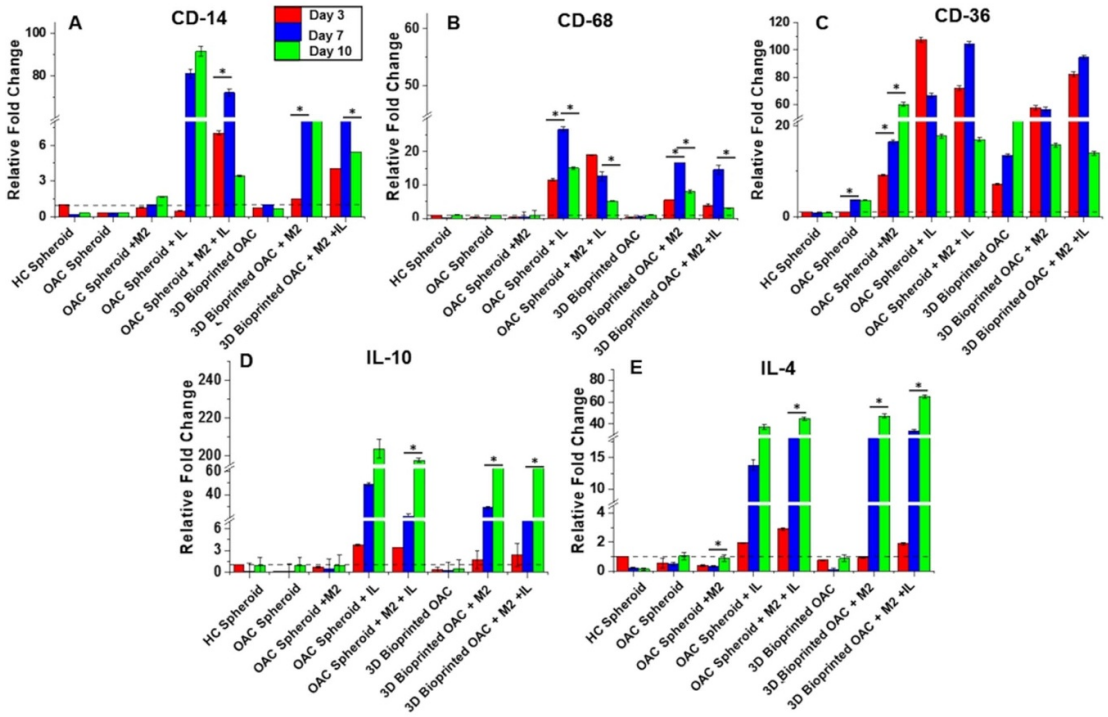

Figure 4. Quantitative real-time PCR to evaluate gene expression of (A) CD-14, (B) CD-36, (C) CD-68, (D) IL-4 and (E) IL-10 at day 3, 7 and 10 of HC spheroids, OAC spheroids, OAC spheroids + IL, OAC spheroids + M2, OAC spheroids + M2 + IL, OAC 3D bioprinted, OAC + M2 3D bioprinted and OAC + M2 + IL 3D bioprinted constructs to evaluate the phenotypic change in the M2 Macrophage. Values are mean ± SD; $n = 3$/group. Symbol * indicates $p < 0.05$ and ** indicates $p < 0.01$." Data normalized to GAPDH.

spheroid group. However, the OAC spheroid + M2 co-culture group exhibited negligible expression of MMP-1 at day 10 (1.62-fold, $p < 0.05$) compared to the only OAC group. The expression of MMP-1 was further decreased 4.52-fold upon the addition of exogenous ILs (OAC spheroids + M2 + IL) against the OAC spheroid + IL group. The 3D bioprinted OAC + M2 model also demonstrated a similar trend with a nominal expression of MMP-1 at day 10 (2.5-fold, $p < 0.05$) against the 3D bioprinted OAC control group. This expression profile was subsequently decreased (3.2-fold) with the addition of the anti-inflammatory ILs (OAC spheroid + IL). The expression levels of MMP-13 for the HC spheroid decreased from day 7 to day 10 (2.21-fold), whereas it increased with increasing time points for the OAC spheroids. Compared to the HC spheroid, a 1.08-fold increase in MMP-13 expression was observed in the OAC spheroid at day 10. However, the 3D bioprinted OAC + M2 co-culture group demonstrated a 1.8-fold decrease in expression of MMP-13 than the OAC spheroid + M2 group at day 10. The anti-inflammatory effect of the exogenously added ILs was corroborated with further downregulation of the MMP-13 expression in the 3D spheroid group. The expression profile of MMP-13 was not affected by the presence or absence of the exogenously added ILs in the 3D bioprinted OAC + M2 group.

3.2.2. Gene expression analysis of M2-specific markers

CD-14 is an established surface marker specific to monocytes that are downregulated upon changes in monocyte plasticity [46]. The expression of this marker will help us to understand if there is any conversion of M2 macrophages to a monocytic state during the culture period in both 3D spheroid and 3D bioprinted culture systems. Nominal expressions of the CD-14 marker were recorded for the HC spheroid, OAC spheroid, and OAC spheroid + IL group (figure 4(A)). Similarly, in the case of OAC spheroid + M2, there was a negligible expression on day 3, which suddenly spiked on day 7 by 80.90-fold ($p < 0.05$). The CD-14 expression level was further elevated at day 10 by 1.13-fold compared to day 7 ($p < 0.05$). However, adding ILs to the OAC spheroid + M2 showed a maximum expression on day 7 (10.27-fold, $p < 0.05$), followed by a sharp decline on day 10. Therefore, a 53-fold increase in CD-14 expression was observed in the OAC spheroid + M2 group at day 10, which further declined 26.7-fold upon exogenous addition of anti-inflammatory ILs. The OAC + M2 3D bioprinted groups also demonstrated a similar trend to the 3D spheroid group with a nominal expression on day 3 followed by a sudden increase at day 7 by 10.19-fold ($p < 0.05$) stable till day 10. The addition of exogenous ILs to the OAC + M2 bioprinted group, however,

downregulated the CD-14 expression from day 7 to day 10 by 10-fold ($p < 0.05$). Thus, when compared at day 10, a 10-fold decrease in CD-14 expression was observed in the 3D bioprinted OAC + M2 + IL group. Therefore, for both the 3D model systems with OAC + M2, evidence of loss in stable M2 macrophage plasticity has been observed that was halted with the addition of exogenous ILs. However, if compared, the 3D bioprinted OAC + M2 group demonstrated a more stable M2 phenotype than the 3D spheroid group, with a 1.78-fold lesser spike in CD-14 expression in the OAC + M2 group without ILs.

CD-36 and **CD-68** are widely recognized as scavenger receptors explicitly expressed on the surface of M1 macrophages [47, 48]. The HC spheroid demonstrated negligible expression of the CD-36 marker, whereas surprisingly, OAC spheroids expressed the CD-36 surface marker, both in the presence and absence of ILs (figure 4(C)). In OAC spheroids, there was a nominal expression at day 3 with a 3.72-fold ($p < 0.05$) upregulation at day 7 that remained stable till day 10. In the presence of ILs, a 6.47-fold ($p < 0.05$) increase in expression was observed on day 7, followed by a 59.7-fold ($p < 0.05$) increase in expression on day 10. Notably, CD-36 expression is correlated with the inflammatory microenvironment devised during the progression of OA via advanced glycation end products that promote cartilage hypertrophy [49, 50]. Moreover, CD-36 also drives inflammation via the advanced glycation of CD36 ligand β-amyloid, thus promoting cartilage matrix catabolism [50–52]. The expression of CD-36 in OAC spheroids + M2 peaked at an initial time point of day 3, which gradually declined at day 10 by 0.26-fold ($p < 0.05$). In the presence of ILs, OAC spheroid + M2 showed elevated expression on day 7 by 1.45-fold ($p < 0.05$) compared to that on day 3, which declined by 0.16-fold ($p < 0.05$) on day 10 compared to that on day 7. Therefore, upon exogenous addition of ILs, a 1.04-fold decrease in the expression of CD-14 was observed in the OAC spheroid + M2 + IL group. The expression levels of CD-36 in the OAC + M2 3D bioprinted group illustrated an increase at initial time points (day 3 and day 7) that was further reduced at day 10 by 3.7-fold and 6.71-fold, respectively, in the presence and absence of ILs. A similar trend was followed by the 3D bioprinted culture group, with a 1.07-fold decrease in CD-36 expression upon IL supplementation at day 10 when compared to the only co-culture counterpart. Similar to the OAC spheroid, the 3D bioprinted OAC group also depicted a characteristic CD-36 expression that increased with increasing time points. Thus, if compared, the expression of CD-36 M1 macrophage receptor was 1.21-fold higher in the 3D spheroid co-culture group with ILs than in the 3D bioprinted group at day 10.

As expected, for the CD-68 M1 surface marker, nominal expression (less than 1-fold change) was observed for HC spheroids, OAC spheroids, OAC spheroids + IL and 3D bioprinted OAC groups (figure 4(B)). The expression of CD-68 in OAC spheroid with ILs increased from day 3 to day 7 by 2.30-fold ($p < 0.05$) and then declined by 0.57-fold ($p < 0.05$) at day 10 compared to day 7. A similar pattern was observed for the OAC + M2 group in the presence of ILs, with a 6.87-fold ($p < 0.05$) increase in expression on day 7 compared to day 3, followed by a subsequent decline by 0.09-fold ($p < 0.05$) on day 10 compared to day 7. Hence, when compared between individual groups, a 15-fold increase in CD-68 expression was observed in OAC spheroid + M2 spheroid, which declined 3-fold upon the addition of anti-inflammatory ILs at day 10. The expression of CD-68 in the OAC + M2 bioprinted construct also showed a 4.31-fold ($p < 0.05$) increase in expression from day 3 to day 7 and then a decline at day 10 by 2.57-fold ($p < 0.05$). However, with the addition of anti-inflammatory ILs, the expression of M1 surface marker CD-68 demonstrated a decline in its expression level from day 7 to day 10 by 1.09-fold ($p < 0.05$). Therefore, a 2.66-fold decline in CD-68 marker expression in the 3D bioprinted OAC + M2 + IL group at day 10 signified the necessity of exogenous IL priming in maintaining M2 plasticity. Thus, for CD-36 and CD-68 marker expressions, the 3D bioprinted co-culture system portrayed an upper hand in conserving the plasticity of the anti-inflammatory M2 macrophage within the co-culture set-up during the entire culture period.

IL-4 and **IL-10** are anti-inflammatory markers predominantly present in M2 macrophage subtypes [36]. There was no expression of IL-4 surface markers in the HC spheroid, OAC spheroid, OAC spheroid + IL, and in the 3D bioprinted OAC group (figures 4(D) and (E)). Elevated expression of IL-4 was observed in OAC spheroid + M2 (4.17-fold, $p < 0.05$), which further increased upon exogenous addition of ILs (9.3-fold $p < 0.05$) at day 10. The 3D bioprinted OAC + M2 group also exhibited a similar tendency with an enhanced level of IL-4 expression at day 10 (5.22-fold, $p < 0.05$) that further escalated with the presence of ILs in the culture media (15.5-fold, $p < 0.05$). For expression of the IL-10 surface marker, there was no expression of IL-10 surface markers in the HC spheroids, OAC spheroids, and OAC spheroids + IL and 3D bioprinted OAC group. The expression level of IL-10 was comparatively higher in the 3D bioprinted OAC + M2 group than in the OAC spheroids + M2 group at day 10 (1.27 times), which further increased with the addition of ILs. The OAC spheroids with M2 macrophages in the absence of ILs showed an 18.98-fold ($p < 0.05$) increase at day 10 from day 3, whereas in 3D bioprinted construct, the expression level was

enhanced by 50.72-fold ($p < 0.05$) when compared to day 3. This trend was further followed even in the presence of ILs, where a 15.5-fold ($p < 0.05$) increase in the level of IL-10 was recorded for the 3D spheroid model, whereas a 36-fold ($p < 0.05$) level of IL-10 expression was observed in 3D bioprinted constructs. Thus, the M2 macrophages in the 3D bioprinted constructs exhibited enhanced anti-inflammatory effects on the cultured OACs, an expected therapeutic outcome while designing a therapeutic strategy for OA.

3.2.3. Gene ontological analysis of the interaction between chondrogenesis and inflammation-related genes

Gene ontological analysis revealed high networking amongst the analyzed genes (COL-I, COL-II, COL-10, MMP-1, MMP-13, CD-14, CD-36, CD-68, IL-4 and IL-10) during chondrogenic differentiation and phenotypic expression of immune cells (supplementary figures 1(A) and (B)). Both chondrogenic genes and surface markers of immune cells displayed intertwined involvement in chondrogenic regeneration, hypertrophy suppression, anti-inflammatory factor upregulation, and pro-inflammatory factor reduction (supplementary figure 1(C)). Additionally, the set of five genes involved in the phenotypic assessment of immune cells aided in depicting their role in the suppression of OA during cartilage regeneration in a 3D co-culture system of spheroid and bioprinted comprising of OAC and M2 macrophages.

3.3. Immunofluorescence study

3.3.1. Protein expression of various collagen types in 3D spheroid and 3D bioprinted model

Using immunofluorescence staining coupled with confocal microscopy, we observed the presence of different types of collagens, such as COL-II and COL-10, as the specific markers of chondrogenesis and hypertrophic differentiation, respectively. HC spheroids showed significant expression of COL-II, which increased from day 3 to day 10 (figure 5). A decrease in COL-II expression in OAC spheroids was recorded, which increased upon exogenous supplementation with ILs from day 3 to day 10. A similar trend was observed for the OAC spheroids + M2 in the presence and absence of ILs. HC spheroids showed no expression of COL-X at either time point; however, increased expression was observed in the OAC spheroids with increasing time points (figure 6). However, in the presence of ILs, the expression in the OAC spheroid subsided from day 3 to day 10. This indicated that anti-inflammatory ILs play a chondroprotective role. A similar trend of COL-X suppression was observed in OAC spheroids + M2 in the absence of ILs. However, in the presence of ILs, there was no effect on the expression of COL-X. In the case of 3D bioprinted OAC constructs, the cell morphology changed from spherical to spindle-shaped, with decreased COL-II expression.

In contrast, similar to our previous findings, COL-X expression increased from day 3 to day 10 in the 3D bioprinted OAC group (figure 7). In the presence of M2 macrophages, with and without ILs, the expression of COL-II increased from day 3 to day 10, but COL-X has minimally expressed in the OA + M2 3D bioprinted constructs even in the presence of ILs. The COL-I expression was not observed in OAC and OAC + M2 3D bioprinted constructs *(Data not shown)*.

3.3.2. Phenotypic changes in M2 macrophages in the OA microcartilage and 3D bioprinted model

The phenotypic changes observed in M2 macrophages upon co-culture with the OAC spheroids were validated by immunoreactivity against specific markers using confocal microscopy. In the presence of ILs, CD-14 expression decreased (figure 8). There was an increase in CD-14 expression from day 3 to day 10 in OAC spheroids + M2 in the absence of ILs, which was reduced in the presence of ILs. OAC spheroids with M2 macrophages showed positive expression of CD-68 surface markers, indicating that M2 macrophages responded positively to the inflammatory 3D OA subtype. Furthermore, an elevated expression of CD-163 was observed in OA spheroids with M2 macrophages and ILs, signifying their synergistic role in directing M2 macrophages to maintain their phenotype during the culture period. We further examined the phenotypic changes observed in M2 macrophages upon co-culture with OAC bioprinted constructs (figure 9). In the presence of exogenous ILs, M2 macrophages retained their morphology and showed a higher expression of CD-163. However, in the absence of ILs, minimal expression of CD-163 was observed.

Moreover, M2 macrophages shed their stable plasticity and convert into monocytes or exhibit M1-like morphology. This was validated with an increase in the expression of CD-14 and CD-68 in the case of OAC + M2 bioprinted constructs. However, there was no to minimal expression of CD-14 and CD-68 OAC + M2 bioprinted constructs in the presence of ILs.

3.4. Biochemical estimation of released cytokines into the medium

During OA progression, various chemokines are produced due to the degradation of HC [53–55]. In addition, macrophages with different polarized states (M1 and M2) may show differential chemokine release in an inflammatory microenvironment [56]. The release profiles of antioxidants and lipid peroxidation were analyzed under all conditions (figure 10). The release of antioxidants among all the experimental groups was the highest for OAC

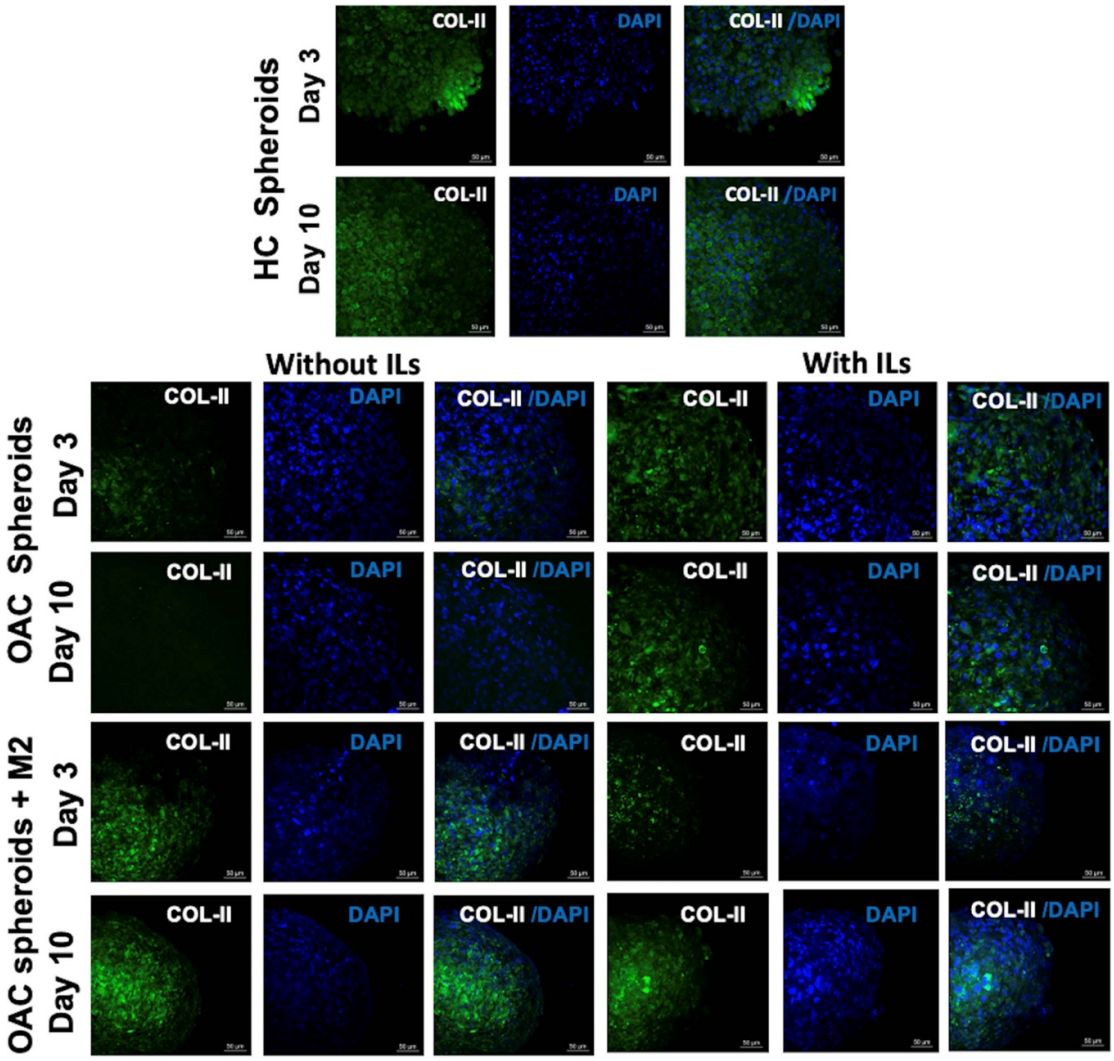

Figure 5. Immunofluorescence analysis depicting the protein expression of COL-II at day 3 and day 10 of HC spheroids, OAC spheroids, OAC spheroids + IL, OAC spheroids + M2, and OAC spheroids + M2 + IL.

spheroids (634.16 ± 29.74 μM) on day 10, which decreased to 499.16 ± 29.17 μM ($p < 0.001$) with the exogenous addition of ILs (figure 10(A)). In contrast, OAC spheroids with M2 macrophages depicted a constant decline in the release of antioxidants with 420.8 ± 13.59 μM on day 3 to 287.4 ± 19.47 μM ($p < 0.001$) on day 10. A similar trend was followed when OAC + M2 spheroids were cultured in the presence of ILs ($p < 0.001$). The release of lipid peroxides and their downstream markers was not significantly different among the conditions. The negligible expression of TBARS indicated no cellular membrane damage in any experimental group, as TBARS is a direct marker of lipid peroxidation (figure 10(B)).

4. Discussion

The onset of OA is marked by progressive cartilage matrix degeneration, inflammation, chondrocyte apoptosis and osteophyte formation with an eventual erosion of articular cartilage tissue within the joint [57]. With the available current treatment modalities, which include pain management therapy in the initial stages and knee arthroplasty in the final stage, developing a phenotypically stable tissue-engineered cartilage implant seemed to be a plausible strategy to mitigate OA. Earlier research from our laboratory has adopted several strategies to regenerate articular cartilage using different combinations of biomaterials and cells [24, 25, 58]. With most investigations centering around developing vivid treatment modalities of OA, the immunogenic molecular mechanism of OA development and mitigation is rarely discussed. Moreover, the role of multiple cell types, like synovial macrophages in advancing and alleviating OA symptoms is often neglected. Our present study explored the advantage of anti-inflammatory M2 macrophages in promoting neo-chondrogenesis while alleviating OA in a co-culture setup comprising of **human primary OACs** and **human M2 macrophages**. We aimed to understand the underlying

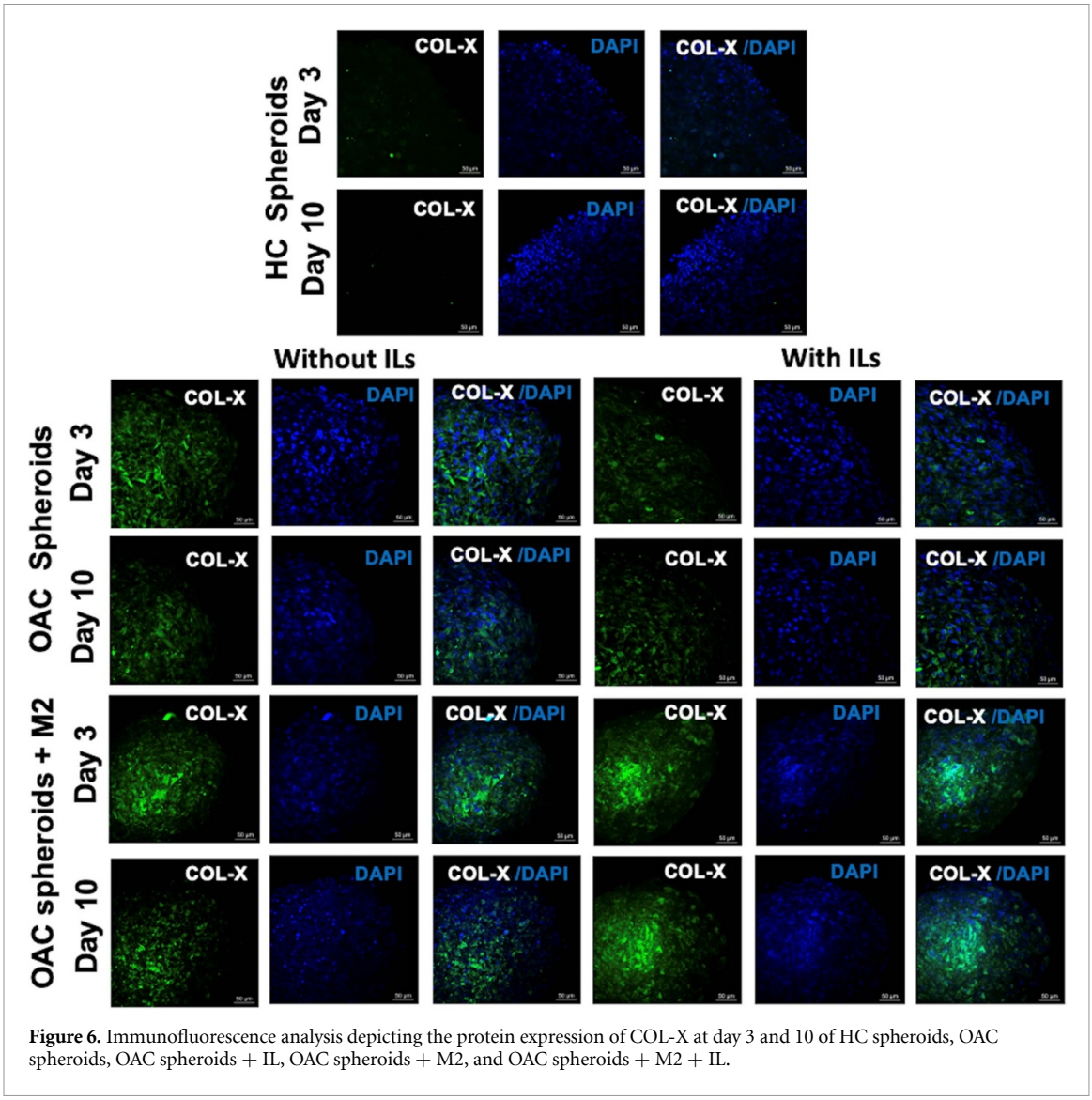

Figure 6. Immunofluorescence analysis depicting the protein expression of COL-X at day 3 and 10 of HC spheroids, OAC spheroids, OAC spheroids + IL, OAC spheroids + M2, and OAC spheroids + M2 + IL.

mechanism of M2 macrophage interaction with the primary human chondrocytes in a 3D spheroid and 3D bioprinted model.

The inter-cellular infiltration and interaction between the diseased articular chondrocytes and anti-inflammatory M2 macrophages was magnificently observed in the 3D OAC microcartilage model using a bright-field microscope. A similar method of M1 macrophage infiltration is observed during the OA inflammation stage with the secretion of pro-inflammatory cytokines (IL-1β, TNF-α), which is gradually replaced by anti-inflammatory M2 macrophages to initiate the remodeling phase, thus contributing to cartilage repair [3, 8, 59]. However, our study, for the first time, depicted the infiltration of the already differentiated M2 macrophage into a diseased chondrocyte microenvironment (OAC spheroid) to initiate healing. When the M2 macrophages were top-seeded onto the OAC spheroids, initially, they appeared scattered around OAC spheroids. As the culture time increased, the immune cells gradually approached the OAC spheroids and initiated direct interaction with their surface (figure 3(E)). The significance of such direct interaction between M2 macrophages and chondrocytes for efficient chondrogenesis has also been elucidated by Kanda *et al* [60]. This direct interaction could be that the cellular migration occurred because of the release of soluble pro-inflammatory factors by the OACs during the culture period that enticed the M2 macrophages to infiltrate toward the OAC spheroid system. Additionally, the M2 macrophages and OACs were directly mixed in a ratio of 10:1 before 3D bioprinting to ensure direct interaction in the 3D bioprinted constructs. An earlier investigation by Samavedi *et al* used transwell-based culture systems to establish the co-culture model of articular chondrocytes and macrophages [30]. However, in such a system, it took almost 72 h for some immune cells to migrate to the bottom of the transwell system and establish communication with the underlying cellular niche [61, 62]. Thus, by the time chondrocytes

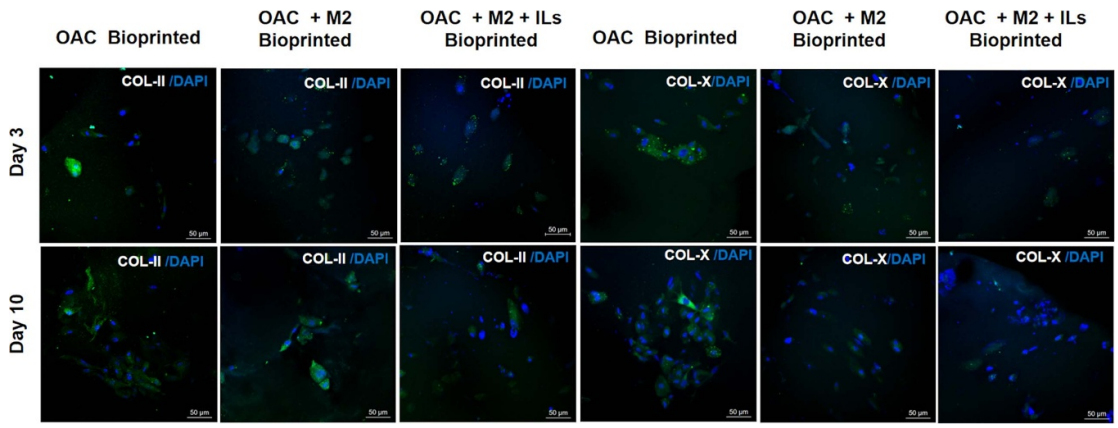

Figure 7. Immunofluorescence analysis depicting the protein expression of COL-II and COL-X in 3D bioprinted constructs.

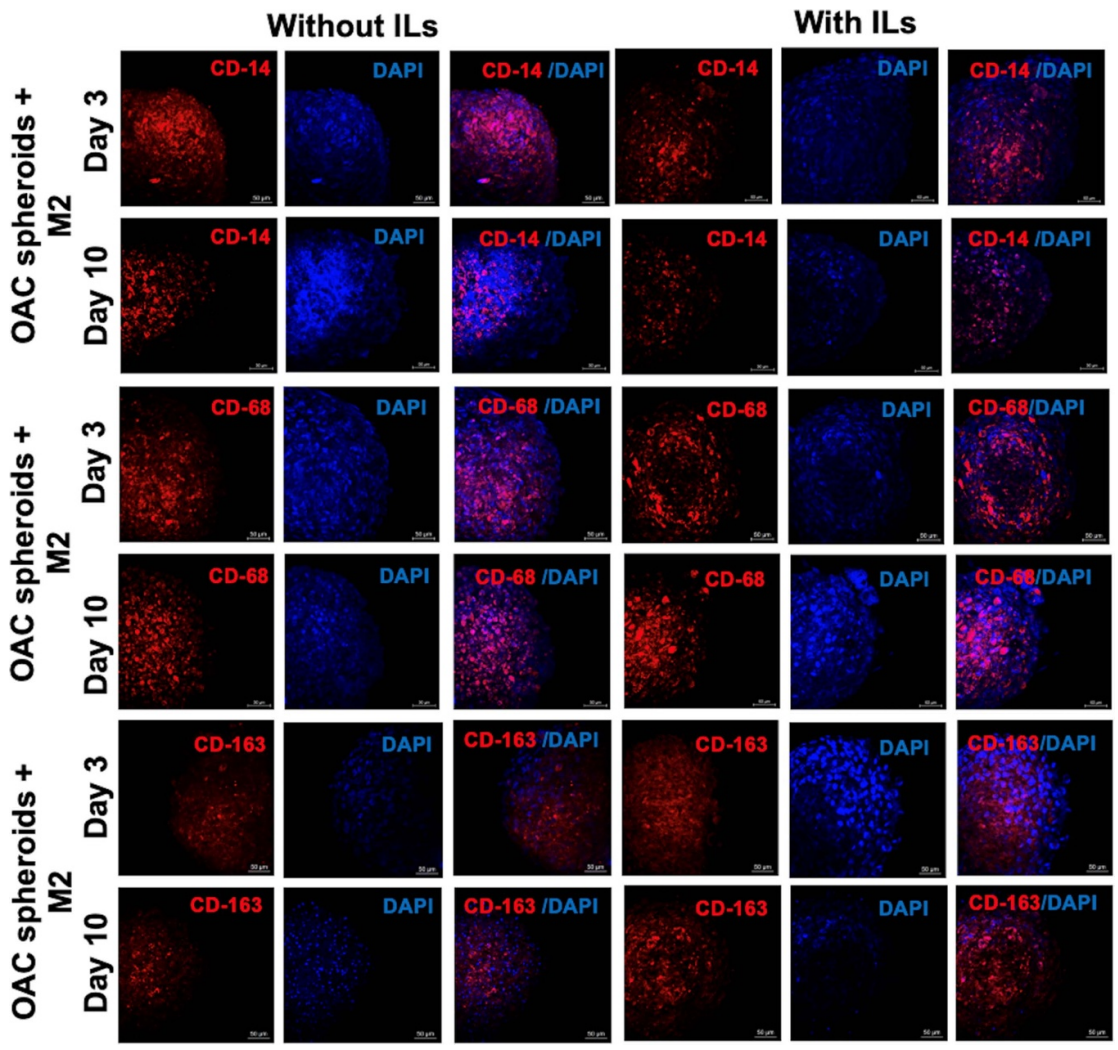

Figure 8. Immunofluorescence analysis depicting the morphological changes using CD-14, CD-68 and CD-163 in the M2 macrophages at days 3 and 10 of OAC spheroids + M2 and OAC spheroids + M2 + IL.

interacted with the macrophages (post 72 h), the immune cells had already started altering their native plasticity in the absence of IL supplementation. Hence, in such a transwell-based system, the effect of the native anti-inflammatory phenotype of M2 macrophage in OA suppression would have been completely obliterated. In our present study, the direct interaction of the M2 macrophages with the OACs

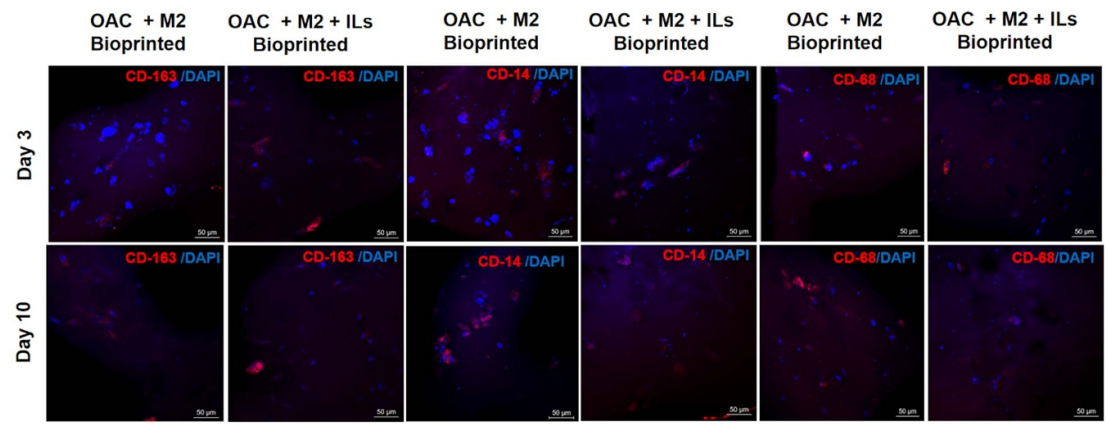

Figure 9. Confocal microscopy depicting morphological changes using CD-14, CD-68 and CD-163 in the M2 macrophages at days 3 and 10 of OAC + M2 and OAC + M2 + IL 3D bioprinted constructs.

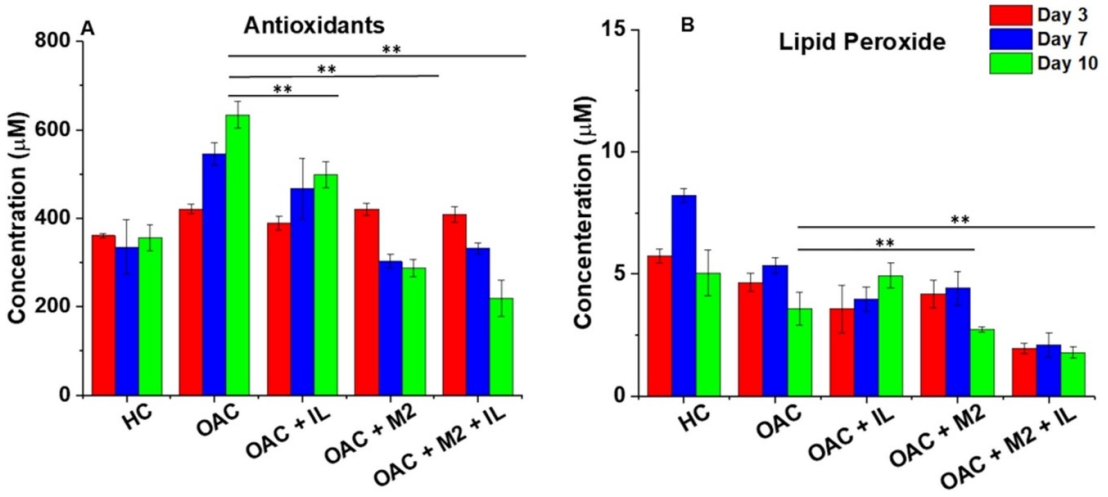

Figure 10. Biochemical estimation of (A) Antioxidants and (B) Lipid peroxidation profile at day 3, 7 and 10 of HC spheroids, OAC spheroids, OAC spheroids + IL, OAC spheroids + M2, and OAC spheroids + M2 + IL. Here, IL is the combination of IL-4 and IL-10. Values are mean ± SD; $n = 3$/group ** indicates $p < 0.001$.

in 3D spheroid and 3D bioprinted models successfully simulated the *in vivo* condition where the M1 macrophages are recruited initially causing inflammation followed by the recruitment of the anti-inflammatory M2 macrophages initiating healing [59, 63].

The next question we aimed to answer was the chondrogenic regeneration potential of the cultured OACs under the influence of anti-inflammatory M2 macrophages. The gene expression data indicated a maximum level of COL-II expression on day 10 for all the experimental groups (figure 3(A)). The former was further validated by protein expression analysis, indicating the excellent chondrogenesis capacity of both the 3D co-culture models in the presence and absence of exogenously added ILs. Therefore, M2 macrophages rightfully promoted neo-chondrogenesis by inducing the expression of pro-chondrogenic TGF-β and IGF genes [63–66]. However, the 3D bioprinted OAC + M2 group depicted an enhanced level of COL-II expression on day 10 than the OAC spheroid + M2 group. This can be attributed to the pro-chondrogenic role of the silk fibroin gelatin microenvironment that additionally enhanced the ability of cartilage regeneration of the OACs in the co-culture model besides the presence of the chondrostimulator M2 macrophages. A detailed proteomics analysis carried out by our research group has earlier demonstrated the activation of the Wnt/β-catenin signaling pathway by the silk-fibroin gelatin bioink that stimulates chondrogenesis *in vitro* [25]. The presence of anti-inflammatory ILs in the culture medium further demonstrated a similar trend but a comparatively lesser level of COL-II expression than without ILs in the 3D bioprinted and 3D spheroid groups. This denotes the chondroprotective effect of ILs in maintaining the healthy phenotype of the chondrocytes [67].

Chondrocyte hypertrophy and ECM degradation are the major hallmark features in OA progression [68, 69]. Cartilage hypertrophy is a long-debated paradigm in articular cartilage development that counteracts chondrocyte maturation [70]. Therefore, to understand the healing mechanism of OA, cartilaginous ECM secretion should be coupled with simultaneous inhibition of hypertrophic differentiation and matrix degradation. Hypertrophic maturation of chondrocytes was analyzed with the expression of COL-I and COL-X, whereas matrix catabolism was evaluated with the expression of MMP-1 and MMP-13 (figures 3(B) and (C)). The expression levels of COL-I declined substantially in the 3D bioprinted OAC + M2 group than in the OAC spheroid + M2, with the OAC spheroid showing the highest expression of the de-differentiation marker at day 10. However, the addition of exogenous ILs significantly alleviated the COL-I expression in both the 3D spheroid and 3D bioprinted models. The COL-X expression in the 3D bioprinted and 3D spheroid co-culture systems was negligible with and without the addition of anti-inflammatory ILs at the latest time point, with the 3D spheroid group showing a comparatively higher expression profile than the 3D bioprinted group. Similarly, the expression profile of matrix catabolism markers MMP-1 and MMP-13 (figures 3(D) and (E)) also displayed a decreasing trend in the OAC + M2 3D spheroid and 3D bioprinted group at day 10 compared to their diseased counterparts (OAC spheroid and 3D bioprinted OAC). Thus, the alternatively activated macrophages post-infiltration have successfully demonstrated their anti-inflammatory and anti-hypertrophic effect by inhibiting matrix catabolism, hypertrophic maturation and chondrocyte dedifferentiation, as already justifying the previous findings by [7, 30, 63]. Furthermore, the declined expression of MMP-13 in the HC spheroid at day 10 than the OAC spheroid can be accounted for the pro-chondrogenic nature of the HC spheroids activating several anabolic cartilage-specific signaling pathways (TGF-β, Wnt/β-catenin). This caused an enhanced chondrogenesis with successful inhibition of expression of matrix degradation protease MMP13. However, the expression profile of MMP-1 for HC spheroids was slightly higher than the OAC spheroid and MMP-13 than the 3D bioprinted OAC group despite the latter two being the diseased group. This can be attributed to the de-differentiation tendency of chondrocytes during monolayer expansion expressing chondrocyte hypertrophy markers (MMP-1 and MMP-13) [71].

Further, we anticipated investigating whether the M2 macrophage can retain its stable anti-inflammatory phenotype or undergo polarization in the co-culture model of 3D spheroids and 3D bioprinted constructs. This was analyzed by studying the gene expression of surface markers (figures 4(A)–(C)) in all experimental sets to validate the morphological changes induced by direct interaction between M2 macrophages and primary chondrocytes. CD-14 is a surface marker widely expressed in human monocytes [46, 72]. It is involved in pattern recognition and simultaneous activation of the immune response in the presence of a foreign body [73, 74]. The increase in the expression of CD-14 in the OAC spheroid + M2 group indicated the polarization of M2 macrophages. In contrast, comparatively less intermediate polarization was observed in the 3D bioprinted OAC + M2 group with a 3-fold lower expression of CD-14 (figure 4(A)). This was further corroborated by the upregulation in the expression pattern of the transition surface marker CD-36 on day 7 in the OAC spheroid + M2 group than the 3D bioprinted co-culture group that was reduced at day 10 (figure 4(C)). The elevated level of CD-36 expression in OAC spheroids (with and without ILs) contributed to the progression of OA marked by the further enhanced expression levels of COL-I, COL-10 and matrix-degrading enzymes MMP-1 and MMP-13 [50]. The expression of the CD-36 marker in these cases can be attributed to the differentiation of M2 macrophages into an M1-like morphology due to the formation of a pro-inflammatory microenvironment due to the OA progression [75]. The expression of pro-inflammatory M1 marker CD-68 exhibited a similar trend with the 3D spheroid co-culture group showing an increased expression pattern than the 3D bioprinted group at day 7, subsiding on day 10 (figure 4(B)). Thus, the tendency of M2 macrophage polarization was higher in the 3D spheroid group than in the 3D bioprinted group. Such stable anti-inflammatory M2 macrophage phenotype was demonstrated by Roy *et al* where the THP-1 monocytes cultured on silk-fibroin material displayed enhanced expression of anti-inflammatory cytokines (IL-4, IL-10 and IL-13) [76]. Thus, our 3D bioprinted constructs with silk matrices supported the stable M2 plasticity superiorly over 3D spheroids. Moreover, the expression profile of all these macrophage polarization surface markers (CD-14, CD-36, and CD-68) showing maximum expression at day 7 and declining on day 10 encourages the development of a pro-inflammatory microenvironment promoting cartilage degradation during the early culture periods. This hypothesis can be further justified with the enhanced expressions of chondrocyte hypertrophy and matrix degradation markers COL-I, COL-X, MMP-1 and MMP-13 at the early time points that sublimed at day 10.

An upregulation in the expression of IL-4 and IL-10 anti-inflammatory ILs has been observed in the 3D spheroid and 3D bioprinted systems throughout the culture period (figures 4(D) and (E)). The cell-mediated maintenance of anti-inflammatory M2 macrophage phenotype and their consecutive role

in OA regulation have been extensively explored by Li *et al* [77]. This indicates healthy proliferation and maintenance of stable M2 macrophage phenotype within the co-culture model in the presence and absence of anti-inflammatory cytokines. Upon exogenous addition of ILs in the culture media, the expression of both IL-4 and IL-10 spiked for both the groups, with the 3D bioprinted constructs exhibiting an upper hand in showing an anti-inflammatory effect. In summary, without cytokine supplementation, a partial population of M2 macrophages in the co-culture tends to lose their native phenotype and convert into M1 macrophage morphology when interacting with OACs. However, in the presence of anti-inflammatory cytokines, maintained M2 macrophages a stable phenotype in the 3D bioprinted group, preferably than the 3D spheroid group [78]. A plausible reason could be the anti-inflammatory environment (expression of IL-4 and IL-10) created by the SF matrices upon culturing THP-1 monocytes on it [76].

Antioxidants help regulate chondrogenesis during the endochondral ossification process [79]. They aid in initiating chondrogenesis in stem cells at the early stages while simultaneously suppressing osteogenic differentiation [80, 81]. However, in chondrocytes, an increased release of antioxidants directs OA pathogenesis. Antioxidant production is strongly controlled by the mitochondrial respiratory chain, oxidative phosphorylation, and NADPH oxidase activity [82]. The maximum antioxidant production was recorded in OAC spheroids, which displayed minimum COL-II and upregulated COL-10 expression. The OAC spheroids + M2 group, however, showed a decline in antioxidant release, which further increased when supplemented with ILs (figure 10). Therefore, the presence of M2 macrophages significantly aided in establishing an anti-inflammatory microenvironment by altering the oxidative defense mechanism, thus demonstrating the onset of OA healing protocol [83, 84].

Therefore, our study successfully illustrated the direct interaction of human OACs and M2 macrophages, resulting in M2-mediated alleviation of OA progression with neo-chondrogenesis. When compared, the 3D bioprinted OAC + M2 macrophage co-culture system portrayed an enhanced arresting capacity of OA progression while promoting chondrogenic re-differentiation than the 3D spheroid culture model despite comprising the same cell number in both the culture groups. Earlier 3D model-based chondrocyte-macrophage coculture studies have used indirect interaction approaches like trans well platforms or macrophage-conditioned media to study the disease development and containment. This study, for the first time, utilized the 3D bioprinting approach, mixing both the cell types together in a 1:10 ratio, establishing direct cell-cell communication besides cell-ECM interaction required for the activation of pro-chondrogenic signaling pathways. Moreover, this study, for the first time, reported the co-culture model of primary human chondrocytes and human-derived M2 macrophages, thereby providing more practical information about the therapeutic effect of the M2-meditated suppression of OA progression in human patients. Additionally, in this study, we have extensively monitored the polarization profile of the cultured macrophages by evaluating their expression pattern of several surface markers during the entire culture period. This information will provide additional information about the stability of the M2 phenotype in the co-culture setup. The supplementation of ILs (IL-4 and IL-10) to the coculture medium further aided in the maintenance of stable anti-inflammatory M2 macrophage phenotype and hindered their de-differentiation to intermediate M0 state. Moreover, this study highlighted the additional advantage of 3D bioprinting using silk-fibroin gelatin bioink in stimulating chondrogenesis in primary OACs besides the chondroprotective role of M2 macrophages in halting the progression of OA when primed in a co-culture setup.

However, overcoming the limitations pertaining to the inclusion of different resident cell types (synoviocytes and osteoblasts) and immune cells (B and T lymphocytes) present in the native OA niche within the coculture setup will more efficiently recapitulate *in vivo* OA pathophysiology. This will broaden our understanding of the regulatory role of various cell types on the OA healing mechanism. A future study can be devised augmenting the advantages of spheroid culture and 3D bioprinting using 3D bioprinting of spheroids consisting of different cell combinations to exemplify further the intricate intracellular and cell-matrix communications besides underlining the molecular signaling pathways governing the cellular infiltration and overall healing process. Such understanding will establish cell-based OA healing therapy as a potential regenerative strategy to contain OA progression.

5. Conclusion

This study recapitulates the human macrophage-mediated OA healing process by focusing on the direct interaction of anti-inflammatory human M2 macrophages into the diseased articular chondrocyte niche (OAC spheroid model), particularly during the remodeling phase of cartilage repair in OA. Additionally, we compared the efficiency of two different 3D co-culture model systems, 3D spheroid-based and 3D bioprinted constructs from human origin, in mitigating OA symptoms while promoting chondrogenesis. The gene expression analysis revealed that the presence of M2 macrophages within

the diseased chondrocyte population significantly alleviated the OA marker expressions as well as promoted the maintenance of stable articular chondrocyte phenotype comparable with the healthy chondrocyte spheroid control. When compared between the experimental groups, the 3D bioprinted system showed enhanced COL-II and downregulated COL-I, COL-X, MMP-1, and MMP-13 than the 3D spheroid co-culture model regardless of containing the same cell population. This inference was further corroborated by protein expression study of COL-I, COL-II, and COL-10 via immunofluorescence analysis, underlining the upper hand of a 3D bioprinted system in stimulating chondrogenic regeneration and curbing OA pathogenesis. Furthermore, the M2 surface marker analysis (CD-14, CD-36, and CD-68) uncovered that the M2 macrophage preferred maintaining its stable anti-inflammatory phenotype in a 3D bioprinted setup, whereas it tended to lose its plasticity towards pro-inflammatory phenotype in OAC spheroid + M2 model. The findings were further confirmed with antioxidant release evaluation, where the 3D bioprinted OAC group with M2 macrophage exemplified a lower release at day 10 than the spheroid counterpart. Thus, the mechanistic crosstalk between the M2 macrophage and the OAC in a 3D bioprinted co-culture system, coupled with the pro-chondrogenic property of silk-fibroin gelatin bioink deliberately reduced the symptoms of OA manifestation, while escalating neo-chondrogenesis. This can be attributed to the cell-ECM interaction within the SF-G bioink that is assumed to activate the already established pro-chondrogenic Wnt/β-catenin signaling pathway while simultaneously inhibiting hypertrophy-inducing IHH pathway. Moreover, when the culture media was supplemented with anti-inflammatory ILs (IL-4 and IL-10), both the 3D models displayed enhanced chondrogenesis, excellent suppression of hypertrophic differentiation and stable M2 phenotype necessitating the chondroprotective role of anti-inflammatory IL-4 and IL-10. Through this study, we have demonstrated for the first time the macrophage-mediated cellular reprogramming of primary human OACs in a 3D bioprinted co-culture system. The findings from this research uncovered the intricate mechanistic details of the direct interaction between the human M2 macrophages and human OACs and the associated OA healing. Thus, this study will be a yardstick for developing a biomaterial-based regenerative therapy containing M2 macrophages for OA. Furthermore, developing a futuristic 3D bioprinted co-culture systems incorporating different other immune cells (T-lymphocytes and B-lymphocytes), osteoblasts, and synoviocytes besides primary human OACs and M2 macrophage within the SF-G biomaterial will successfully recapitulate the native healing OA microenvironment *in vitro* required for understanding the underlying mechanism for complete suppression of OA progression.

Data availability statements

The data cannot be made publicly available upon publication because the cost of preparing, depositing and hosting the data would be prohibitive within the terms of this research project. The data that support the findings of this study are available upon reasonable request from the authors.

Declarations

The authors declare no competing financial interests or personal relationships that could influence the work reported in this study.

Ethics approval and consent of participation

Isolation of human chondrocytes from human cartilage: a single-center prospective pilot study. IEC application No- IAH-BMR-018/10-19

Conflict of interest

All the authors declare no potential conflict of interest.

Funding

Department of Biotechnology India-Swiss project (BT/IN/Swiss/54/SG/2018-19).

ORCID iDs

Subhadeep Roy https://orcid.org/0000-0002-0805-2505
Sourabh Ghosh https://orcid.org/0000-0002-1091-9614

References

[1] Roberts S, Genever P, McCaskie A B C and Bari C D 2011 Prospects of stem cell therapy in osteoarthritis *Regen. Med.* **6** 351–66
[2] Katz J N, Earp B E and Gomoll A H 2010 Surgical management of osteoarthritis *Arthritis Care Res.* **62** 1220–8
[3] Woodell-May J E and Sommerfeld S D 2020 Role of inflammation and the immune system in the progression of osteoarthritis *J. Orthop. Res.* **38** 253–7
[4] Murray P J and Wynn T A 2011 Protective and pathogenic functions of macrophage subsets *Nat. Rev. Immunol.* **11** 723–37
[5] Ma Y *et al* 2021 Artificial M2 macrophages for disease-modifying osteoarthritis therapeutics *Biomaterials* **274** 120865
[6] Ummarino A, Gambaro F M, Kon E and Torres Andón F 2020 Therapeutic manipulation of macrophages using

nanotechnological approaches forthe treatment of osteoarthritis *Nanomaterials* **10** 1562
[7] Chen Y, Jiang W, Yong H, He M, Yang Y, Deng Z and Li Y 2020 Macrophages in osteoarthritis: pathophysiology and therapeutics *Am. J. Transl. Res.* **12** 261–8
[8] Fernandes T L, Gomoll A H, Lattermann C, Hernandez A J, Bueno D F and Amano M T 2020 Macrophage: a potential target on cartilage regeneration *Front. Immunol.* **11** 111
[9] Davis M J, Tsang T M, Qiu Y, Dayrit J K, Freij J B, Huffnagle G B, Olszewski M A and Dromer F 2013 Macrophage M1/M2 polarization dynamically adapts to changes in cytokine microenvironments in Cryptococcus neoformans infection *mBio* **4** e00264–13
[10] Hoeffel G and Ginhoux F 2018 Fetal monocytes and the origins of tissue-resident macrophages *Cell Immunol.* **330** 5–15
[11] Gu Q, Yang H and Shi Q 2017 Macrophages and bone inflammation *J. Orthop. Translat.* **10** 86
[12] Madsen D H *et al* 2013 M2-like macrophages are responsible for collagen degradation through a mannose receptor–mediated pathway *J. Cell Biol.* **202** 951
[13] Ghosh S, Parker S T, Wang X, Kaplan D L and Lewis J A 2008 Direct-write assembly of microperiodic silk fibroin scaffolds for tissue engineering applications *Adv. Funct. Mater.* **18** 1883–9
[14] la Flamme A C, Kharkrang M, Stone S, Mirmoeini S, Chuluundorj D, Kyle R and Bereswill S 2012 Type II-activated murine macrophages produce IL-4 *PLoS One* **7** e46989
[15] da Silva M D, Bobinski F, Sato K L, Kolker S J, Sluka K A and Santos A R S 2015 IL-10 cytokine released from M2 macrophages is crucial for analgesic and anti-inflammatory effects of acupuncture in a model of inflammatory muscle pain *Mol. Neurobiol.* **51** 19–31
[16] Doyle A G, Herbein G, Montaner L J, Minty A J, Caput D, Ferrara P and Gordon S 1994 Interleukin-13 alters the activation state of murine macrophages *in vitro*: comparison with interleukin-4 and interferon-γ *Eur. J. Immunol.* **24** 1441–5
[17] Wu C-L, Harasymowicz N S, Klimak M A, Collins K H and G F 2020 The role of macrophages in osteoarthritis and cartilage repair *Osteoarthr. Cartil.* **28** 544–54
[18] Liu B, Zhang M, Zhao J, Zheng M and Yang H 2018 Imbalance of M1/M2 macrophages is linked to severity level of kneeosteoarthritis *Exp. Ther. Med.* **16** 5009–14
[19] Brigitte M, Schilte C, Plonquet A, Baba-Amer Y, Henri A, Charlier C, Tajbakhsh S, Albert M, Gherardi R K and Chrétien F 2010 Muscle resident macrophages control the immune cell reaction in a mouse model of notexin-induced myoinjury *Arthritis Rheumatol.* **62** 268–79
[20] Louwe P, Badiola Gomez L, Webster H, Perona-Wright G, Bain C, Forbes S J S and Jenkins S J 2021 Recruited macrophages that colonize the post-inflammatory peritoneal niche convert into functionally divergent resident cells *Nat. Commun.* **12** 1–15
[21] Chawla S, Midha S, Sharma A and Ghosh S 2018 Silk-based bioinks for 3D bioprinting *Adv. Healthcare Mater.* **7** 1701204
[22] Das S, Pati F, Chameettachal S, Pahwa S, Ray A R, Dhara S and Ghosh S 2013 Enhanced redifferentiation of chondrocytes on microperiodic silk/gelatin scaffolds: toward tailor-made tissue engineering *Biomacromolecules* **14** 311–21
[23] Das S, Pati F, Choi Y-J, Rijal G, Shim J-H, Kim S W, Ray A R, Cho D-W and Ghosh S 2015 Bioprintable, cell-laden silk fibroin-gelatin hydrogel supporting multilineage differentiation of stem cells for fabrication of three-dimensional tissue constructs *Acta Biomater.* **11** 233–46
[24] Chameettachal S, Midha S and Ghosh S 2016 Regulation of chondrogenesis and hypertrophy in silk fibroin-gelatin-based 3D bioprinted constructs *ACS Biomater. Sci. Eng.* **2** 1450–63
[25] Chawla S, Desando G, Gabusi E, Sharma A, Trucco D, Chakraborty J, Manferdini C, Petretta M, Lisignoli G and Ghosh S 2021 The effect of silk–gelatin bioink and TGF-β3 on mesenchymal stromal cells in 3D bioprinted chondrogenic constructs: a proteomic study *J. Mater. Res.* **36** 4051–67
[26] Chakraborty J and Ghosh S 2020 Cellular proliferation, self-assembly, and modulation of signaling pathways in silk fibroin gelatin-based 3D bioprinted constructs *ACS Appl. Bio Mater.* **3** 8309–20
[27] Bhattacharjee M, Coburn J, Centola M, Murab S, Barbero A, Kaplan D L, Martin I and Ghosh S 2015 Tissue engineering strategies to study cartilage development, degeneration and regeneration *Adv. Drug Deliv. Rev.* **84** 107–22
[28] Sun L, Wang X and Kaplan D L 2011 A 3D cartilage—inflammatory cell culture system for the modeling of humanosteoarthritis *Biomaterials* **32** 5581–9
[29] Fujihara Y, Abe T and Hoshi K 2020 Controlling the phenotype of macrophages promotes maturation of tissue-engineeredCartilage *Tissue Eng.* A **26** 1005–13
[30] Samavedi S, Diaz-Rodriguez P, Erndt-Marino J D and Hahn M S 2017 A three-dimensional chondrocyte-macrophage coculture system to probe inflammation in experimental osteoarthritis *Tissue Eng.* A **23** 101–14
[31] Murphy C L and Polak J M 2004 Control of human articular chondrocyte differentiation by reduced oxygen tension *J. Cell Physiol.* **199** 451–9
[32] Sasazaki Y, Seedhom B B and Shore R 2008 Morphology of the bovine chondrocyte and of its cytoskeleton in isolation and in situ: are chondrocytes ubiquitously paired through the entire layer of articular cartilage? *Rheumatology* **47** 1641–6
[33] Chawla S, Kumar A, Admane P, Bandyopadhyay A and Ghosh S 2017 Elucidating role of silk-gelatin bioink to recapitulate articular cartilage differentiation in 3D bioprinted constructs *Bioprinting* **7** 1–13
[34] Chawla S, Berkelaar M H M, Dasen B, Halleux C, Guth-Gundel S, Kramer I, Ghosh S, Martin I, Barbero A and Occhetta P 2020 Blockage of bone morphogenetic protein signalling counteracts hypertrophy in a human osteoarthritic micro-cartilage model *J. Cell Sci.* **133** jcs249094
[35] Hamada T, Sakai T, Hiraiwa H, Nakashima M, Ono Y, Mitsuyama H and Ishiguro N 2013 Surface markers and gene expression to characterize the differentiation of monolayer expanded human articular chondrocytes *Nagoya J. Med. Sci.* **75** 101
[36] Mantovani A, Sica A, Sozzani S, Allavena P, Vecchi A and Locati M 2004 The chemokine system in diverse forms of macrophage activation and polarization *Trends Immunol.* **25** 677–86
[37] Bhattacharjee M, Chawla S, Chameettachal S, Murab S, Bhavesh N S and Ghosh S 2016 Role of chondroitin sulphate tethered silk scaffold in cartilaginous disc tissue regeneration *Biomed. Mater.* **11** 25014
[38] Murab S, Samal J, Shrivastava A, Ray A R, Pandit A and Ghosh S 2015 Glucosamine loaded injectable silk-in-silk integrated system modulate mechanical properties in bovine *ex-vivo* degenerated intervertebral disc model *Biomaterials* **55** 64–83
[39] Chawla S, Sharma A, Bandyopadhyay A and Ghosh S 2018 Developmental biology-inspired strategies to engineer 3D bioprinted bone construct *ACS Biomater. Sci. Eng.* **4** 3545–60
[40] Majumder N, Mishra A and Ghosh S 2022 Effect of varying cell densities on the rheological properties of the bioink *Bioprinting* **28** e00241
[41] Fujihara Y, Takato T and Hoshi K 2014 Macrophage-inducing FasL on chondrocytes forms immune privilege in cartilage tissue engineering, enhancing *in vivo* regeneration *Stem Cells* **32** 1208–19
[42] Banerjee S, Roy S, Bhaumik K N and Pillai J 2020 Mechanisms of the effectiveness of lipid nanoparticle formulations loaded with anti-tubercular drugs combinations toward overcoming drug bioavailability in tuberculosis *J. Drug Target* **28** 55–69

[43] Chakraborty J et al 2019 Modulation of macrophage phenotype, maturation, and graft integration through chondroitin sulfate cross-linking to decellularized cornea *ACS Biomater. Sci. Eng.* **5** 165–79
[44] Roy S et al 2018 GLA supplementation regulates PHD2 mediated hypoxia and mitochondrial apoptosis in DMBA induced mammary gland carcinoma *Int. J. Biochem. Cell Biol.* **96** 51–62
[45] Roy S et al 2017 Alpha-linolenic acid stabilizes HIF-1 α and downregulates FASN to promote mitochondrial apoptosis for mammary gland chemoprevention *Oncotarget* **8** 70049
[46] Steinbach F and Thiele B 1994 Phenotypic investigation of mononuclear phagocytes by flow cytometry *J. Immunol. Methods* **174** 109–22
[47] Minami K et al 2018 Prognostic significance of CD68, CD163 and Folate receptor-β positive macrophages in hepatocellular carcinoma *Exp. Ther. Med.* **15** 4465
[48] Tontonoz P, Nagy L, Alvarez J G A, Thomazy V A and Evans R M 1998 PPARgamma promotes monocyte/macrophage differentiation and uptake of oxidized LDL *Cell* **93** 241–52
[49] Podrez E A, Febbraio M, Sheibani N, Schmitt D, Silverstein R L, Hajjar D P, Cohen P A, Frazier W A, Hoff H F and Hazen S L 2000 Macrophage scavenger receptor CD36 is the major receptor for LDL modified by monocyte-generated reactive nitrogen species *J. Clin. Invest.* **105** 1095–108
[50] Cecil D L, Appleton C T G, Polewski M D, Mort J S, Schmidt A M, Bendele A, Beier F and Terkeltaub R 2009 The pattern recognition receptor CD36 is a chondrocyte hypertrophy marker associated with suppression of catabolic responses and promotion of repair responses to inflammatory stimuli *J. Immunol.* **182** 5024
[51] Moore K J, El Khoury J, Medeiros L A, Terada K, Geula C, Luster A D and Freeman M W 2002 A CD36-initiated signaling cascade mediates inflammatory effects of beta-amyloid *J. Biol. Chem.* **277** 47373–9
[52] El Khoury J B, Moore K J, Means T K, Leung J, Terada K, Toft M, Freeman M W and Luster A D 2003 CD36 mediates the innate host response to beta-amyloid *J. Exp. Med.* **197** 1657–66
[53] Lotz M 1999 The role of nitric oxide in articular cartilage damage *Rheum Dis. Clin. North Am.* **25** 269–82
[54] Tiku M L, Gupta S and Deshmukh D R 1999 Aggrecan degradation in chondrocytes is mediated by reactive oxygen species and protected by antioxidants *Free Radic. Res.* **30** 395–405
[55] Villalvilla A, Gómez R, Largo R and Herrero-Beaumont G 2013 Lipid transport and metabolism in healthy and osteoarthritic cartilage *Int. J. Mol. Sci.* **14** 20793
[56] Ruytinx P, Proost P, Van Damme J and Struyf S 2018 Chemokine-induced macrophage polarization in inflammatory conditions *Front. Immunol.* **9** 1930
[57] Lotz M K, Otsuki S, Grogan S P, Sah R, Terkeltaub R and D'Lima D 2010 Cartilage cell clusters *Arthritis Rheumatol.* **62** 2206–18
[58] Chakraborty J, Majumder N, Sharma A, Prasad S and Ghosh S 2022 3D bioprinted silk-reinforced alginate-gellan gum constructs for cartilage regeneration *Bioprinting* **28** e00232
[59] Sanchez-Lopez E, Coras R, Torres A, Lane N E and Guma M 2022 Synovial inflammation in osteoarthritis progression *Nat. Rev. Rheumatol.* **18** 258–75
[60] Kanda K, Asawa Y, Inaki R, Fujihara Y, Hoshi K and Hikita A 2021 Requirement of direct contact between chondrocytes and macrophages for the maturation of regenerative cartilage *Sci. Rep.* **11** 22476
[61] Lindholm P F, Lu Y, Adley B P, Vladislav T, Jovanovic B, Sivapurapu N, Yang X J and Kajdacsy-Balla A 2010 Role of monocyte-lineage cells in prostate cancer cell invasion and tissue factor expression *Prostate* **70** 1672–82
[62] Coburn P T, Herbay A C, Berrini M and Li-Jessen Nicole Y K 2021 An *in vitro* assessment of the response of THP-1 macrophages to varying stiffness of a glycol-chitosan hydrogel for vocal fold tissue engineering applications *J. Biomed. Mater. Res.* A **109** 1337–52
[63] Zhu X, Lee C-W, Xu H, Wang Y-F, Yung P S H, Jiang Y and Lee O K 2021 Phenotypic alteration of macrophages during osteoarthritis: a systematic review *Arthritis Res. Ther.* **23** 110
[64] Zhang H, Cai D and Bai X 2020 Macrophages regulate the progression of osteoarthritis *Osteoarthr. Cartil.* **28** 555–61
[65] Dai M, Sui B, Xue Y, Liu X and Sun J 2018 Cartilage repair in degenerative osteoarthritis mediated by squid type IIcollagen via immunomodulating activation of M2 macrophages,inhibiting apoptosis and hypertrophy of chondrocytes *Biomaterials* **180** 91–103
[66] Pan X, Yuan S, Xun X, Fan Z, Xue X, Zhang C, Wang J and Deng J 2022 Long-term recruitment of endogenous M2 macrophages by platelet lysate-rich plasma macroporous hydrogel scaffold for articular cartilage defect repair *Adv. Healthcare Mater.* **11** 2101661
[67] Wojdasiewicz P, Poniatowski Ł A and Szukiewicz D 2014 The role of inflammatory and anti-inflammatory cytokines in the pathogenesis of osteoarthritis *Mediators Inflamm.* **2014** 1–19
[68] Majumder N and Ghosh S 2023 Unfolding the mystery behind the onset of chondrocyte hypertrophy during chondrogenesis: toward designing advanced permanent cartilage-mimetic biomaterials *Adv. Funct. Mater.* **33** 2300651
[69] Chawla S et al 2022 Chondrocyte hypertrophy in osteoarthritis: mechanistic studies and models for theidentification of new therapeutic strategies *Cells* **11** 4034
[70] Drissi H, Zuscik M, Rosier R and O'Keefe R 2005 Transcriptional regulation of chondrocyte maturation: potential involvement of transcription factors in OA pathogenesis *Mol. Aspects Med.* **26** 169–79
[71] Charlier E, Deroyer C, Ciregia F, Malaise O, Neuville S, Plener Z, Malaise M and de Seny D 2019 Chondrocyte dedifferentiation and osteoarthritis (OA) *Biochem. Pharmacol.* **165** 49–65
[72] Landmann R, Müller B and Zimmerli W 2000 CD14, new aspects of ligand and signal diversity *Microbes Infect.* **2** 295–304
[73] Antal-Szalmas P, Van Strijp J A G, Weersink A J L, Verhoef J and Van Kessel K P M 1997 Quantitation of surface CD14 on human monocytes and neutrophils *J. Leukoc. Biol.* **61** 721–8
[74] Bufler P, Stiegler G, Schuchmann M, Hess S, Krüger C, Stelter F, Eckerskorn C, Schütt C and Engelmann H 1995 Soluble lipopolysaccharide receptor (CD14) is released via two different mechanisms from human monocytes and CD14 transfectants *Eur. J. Immunol.* **25** 604–10
[75] Cecil D L, Johnson K, Rediske J, Lotz M, Schmidt A M and Terkeltaub R 2005 Inflammation-induced chondrocyte hypertrophy is driven by receptor for advanced glycation end products *J. Immunol.* **175** 8296–302
[76] Roy S, Sharma A and Ghosh S 2022 Macrophage polarization profiling on native and regenerated silk biomaterials *ACS Biomater. Sci. Eng.* **8** 659–71
[77] Li K et al 2022 Anti-inflammatory and immunomodulatory effects of the extracellular vesicles derived from human umbilical cord mesenchymal stem cells on osteoarthritis via M2 macrophages *J. Nanobiotechnol.* **20** 38
[78] Wynn T A and Barron L 2010 Macrophages: master regulators of inflammation and fibrosis *Semin. Liver Dis.* **30** 245–57
[79] Yanes O, Clark J, Wong D M, Patti G J, Sánchez-Ruiz A, Benton H P, Trauger S A, Desponts C, Ding S and Siuzdak G 2010 Metabolic oxidation regulates embryonic stem cell differentiation *Nat. Chem. Biol.* **6** 411–7
[80] Chen C-T, Shih Y-R V, Kuo T K, Lee O K and Wei Y-H 2008 Coordinated changes of mitochondrial biogenesis and antioxidant enzymes during osteogenic differentiation of human mesenchymal stem cells *Stem Cells* **26** 960–8
[81] Ki S K, Hae W C, Hee E Y and Ick Y K 2010 Reactive oxygen species generated by NADPH oxidase 2 and 4 are required for chondrogenic differentiation *J. Biol. Chem.* **285** 40294

[82] Minguzzi M, Cetrullo S, D'Adamo S, Silvestri Y, Flamigni F and Borzì R M 2018 Emerging players at the intersection of chondrocyte loss of maturational arrest, oxidative stress, senescence and low-grade inflammation in osteoarthritis *Oxid. Med. Cell. Longev.* **2018** 1–17

[83] Virág L, Jaén R I, Regdon Z, Boscá L and Prieto P 2019 Self-defense of macrophages against oxidative injury: fighting for their ownsurvival *Redox Biol.* **26** 101261

[84] Pérez S and Rius-Pérez S 2022 Macrophage polarization and reprogramming in acute inflammation: a redox perspective *Antioxidants* **11** 1394